

Crossing the cosmological constant barrier with kinetically interacting double quintessence

Sourav Sur

Dept. of Physics, University of Lethbridge
4401 University Drive, Lethbridge, Alberta, Canada T1K 3M4

E-mail: sourav.sur@uleth.ca

Abstract. We examine the plausibility of crossing the cosmological constant (Λ) barrier in a two-field quintessence model of dark energy, involving a kinetic interaction between the individual fields. Such a kinetic interaction may have its origin in the four dimensional effective two-field version of the Dirac-Born-Infeld action, that describes the motion of a D3-brane in a higher dimensional space-time. We show that this interaction term could indeed enable the dark energy equation of state parameter w_x to cross the Λ -barrier (i.e., $w_x = -1$), keeping the Hamiltonian well behaved (bounded from below), as well as satisfying the condition of stability of cosmological density perturbations, i.e., the positivity of the squares of the sound speeds corresponding to the adiabatic and entropy modes. The model is found to fit well with the latest Supernova Union data and the WMAP results. The best fit curve for w_x crosses -1 at red-shift z in the range $\sim 0.215 - 0.245$, whereas the transition from deceleration to acceleration takes place in the range of $z \sim 0.56 - 0.6$. The scalar potential reconstructed using the best fit model parameters is found to vary smoothly with time, while the dark energy density nearly follows the matter density at early epochs, becomes dominant in recent past, and slowly increases thereafter without giving rise to singularities in finite future.

PACS numbers: 98.80.-k, 95.36.+x, 98.80.JK

1. Introduction

A variety of recent observational probes, including in particular the type Ia Supernovae (SN Ia) [1, 2, 3, 4, 5, 6, 7, 8, 9], indicate that our universe has entered in a phase of accelerated expansion in recent past, following an early decelerating regime. Despite several alternative proposals, such as modified gravity [10] and the averaging of cosmological inhomogeneities [11], the origin of this acceleration has widely been attributed to a ‘mysterious’ energy component, namely the dark energy (DE), which constitutes about 72% of the present universe. Moreover, the cosmic microwave background (CMB) temperature fluctuation measurements by the Wilkinson Microwave Anisotropy Probe (WMAP) [12, 13, 14] as well as the large scale red-shift data from the Sloan Digital Sky Survey (SDSS) [15] indicate that our universe is very nearly spatially flat, so that spatial inhomogeneities may be neglected at large scales. Although the DE closely resembles a positive cosmological constant Λ , for which the DE equation of state (EoS) parameter $w_x = -1$, there are some serious theoretical problems, such as *fine tuning* and *coincidence*, associated with Λ [16]. Specifically, if the DE is supposed to be due to Λ and the acceleration began only in recent past, then (i) what makes the DE density scale very small compared to the Planck scale? and (ii) why is the DE density ρ_x is of the order of the present critical density ρ_{oc} right now? Hence, there have been suggestions that the DE may be (more appropriately) *dynamic* and can be modeled by one or more scalar field(s) originating from a fundamental theory. Of major interest are the DE models developed in the framework of quintessence and tracker fields [17, 18], k-essence [19, 20], Chaplygin gas [21] etc., (see [22] for extensive reviews). However, in many of these models the value of w_x is always restricted to be ≥ -1 , which is not desirable for a consistent statistical fit with the observational data. In fact, even with the presumption that w_x is a constant, the recent WMAP five year data, combined with those for SN Ia and baryon acoustic oscillation (BAO) peaks, constrain the value of $1 + w_x$, to be between -0.14 and 0.12 , at 95% confidence level (CL) [14]. For a time-varying DE, the same data constrain the value w_{ox} of the DE EoS parameter at the present epoch (i.e., at red-shift $z = 0$) to be between -1.33 and 0.79 (at 95% CL) [14]. Since in the distant past, the value of a variable w_x must have to be $\gg -1$ (so that the universe had a decelerated expansion and structures were formed), there is a fair plausibility that one (or possibly more) transition(s) from $w_x > -1$ to $w_x < -1$ (or vice versa) could have been taken place in the recent course of evolution of the DE, and at present $w_x = w_{ox} < -1$.

The crossing of the cosmological constant barrier ($w_x = -1$) can, most simply, be achieved in the so-called *quintom* scenario [23], where there are two (or more) scalar fields, (at least) one of which is of ‘phantom’ nature, i.e., carries a wrong sign in front of the kinetic term in the Lagrangian [24]. Such a phantom field is quantum mechanically unstable [25] and also gives rise to singularities in finite future [26, 27]. Moreover, classical instabilities could arise as the dominant energy condition gets violated in the models involving the phantom fields [28]. Attempts have therefore been made to circumvent the problem of $w_x = -1$ crossing in various alternative ways. Notable among these are the scalar-tensor models [29], brane-world models [30], multi-field k-essence models [31, 32], modified gravity models [33], string-inspired dilatonic ghost condensate models [34], quantum-corrected Klein-Gordon models with quartic potential

[35], coupled DE models [36], H-essence (complex scalar) models [37], etc. However, apart from a very few exceptions (such as the scalar-tensor models [29], or models where the kinetic term abruptly flips sign due to some extraordinary nature of the potential [38]) the $w_x = -1$ crossing is hard to be realized with a single-field DE. Even in the case of a single-field k-essence DE, with a generic non-linear dependence of the Lagrangian on the kinetic term, such a crossing either leads to instabilities against cosmological perturbations or is realized by a discrete set of phase space trajectories[‡] [40]. In multi-field DE models, however, the $w_x = -1$ crossing could be made possible, as is shown for example in refs. [31, 32], although the field configuration may be severely constrained by the criterion of stability, i.e., the square of the effective speed of propagation of cosmological perturbations should be positive definite [32].

In this paper we explore the plausibility of the Λ -barrier crossing in the framework of a two-field quintessence model with a kinetic interaction between the individual fields. Such a model may be looked upon as a specialization of a more general (interacting) multi-field k-essence scenario, which involves non-canonical (higher order) kinetic terms for the scalar fields [19, 32, 41, 42, 43]. Moreover, the kinetically interacting double quintessence (KIDQ) Lagrangian may, under certain approximations, be derived from the four dimensional effective two-field version of the Dirac-Born-Infeld (DBI) Lagrangian describing the evolution of D3-branes in higher dimensional string theoretic manifolds [44]. The biggest advantage with such a Lagrangian, compared to those in other Λ -barrier crossing multiple k-essence models [31, 32], is that the total DE Hamiltonian consists of a positive definite kinetic part, which ensures that it is bounded from below and the model is quantum mechanically consistent. Stability against cosmological density perturbations further requires the squares of the effective (sound) speeds of propagation of the adiabatic and entropy modes to be positive definite as well. For the DBI multiple scalar fields in homogeneous cosmological backgrounds, both these sound speeds turn out to be the same, implying isotropic propagation of the adiabatic and entropy modes [41, 42]. Assuming this result to hold approximately for KIDQ (which is an approximation to the DBI two-scalar scenario), we find the square of the effective (isotropic) sound speed to be positive definite, ensuring the stability of the KIDQ model[§].

We consider certain specific ansatze to solve for the KIDQ field equations, and obtain the condition under which the $w_x = -1$ line could be crossed in some regime. In choosing the ansatze, we particularly emphasize on the following:

- (i) the kinetic energy densities of the interacting scalar fields should always be positive definite,
- (ii) the DE density should be less but not very smaller than the matter density at early epochs, and should dominate the latter at late times, and
- (iii) the DE density should not grow rapidly with increasing scale factor a (i.e., decreasing red-shift z) and reach to abnormally high values in finite future.

[‡] Of course, there are exceptions as well, see for example ref. [39].

[§] More precisely, however, there is a splitting between the propagation speeds of the adiabatic and the entropy modes, when the KIDQ is taken to be an exact theory (not an approximation to DBI). This we find in a subsequent paper [45] (in preparation) by carrying out the stability analysis for KIDQ, following the general formalism worked out in refs. [42, 43] in the context of multi-field DBI and k-inflation. The squares of the propagation speeds turn out to be positive definite anyway.

These are important in order to avoid (i) ghosts or phantoms, (ii) coincidence or fine-tuning related problems, and (iii) occurrence of future singularities, respectively.

We then constrain the parameters of the model with the latest Supernova Ia data compiled in ref. [8], viz., the 307 Union data-set, as well as with the WMAP 5-year [14] update of the CMB-shift parameter \mathcal{R} and the scalar spectral index n_s , which determines the BAO peak distance parameter \mathcal{A} from the SDSS luminous red galactic distribution [15]. After uniformly marginalizing over the Hubble constant H_0 , we obtain good fits of the model with the data. The minimized value of the total χ^2 (SN+CMB+BAO) is found to be $\simeq 311$, which is better than the minimized χ^2 ($\simeq 313$) found with the Union data-set in ref. [9] for the cosmological constant DE coupled with cold dark matter – the so-called Λ CDM model. The best fit values of the parameters of our KIDQ model indicate that the crossing from $w_x > -1$ to $w_x < -1$ takes place at a red-shift range $0.215 \leq z_c \leq 0.245$, whereas the transition from the decelerated regime to the accelerated regime occurs in the range $0.562 \leq z_t \leq 0.603$. At the present epoch ($z = 0$), the best fit values of the matter density parameter and the DE EoS parameter, are respectively found to lie within the ranges $0.279 \leq \Omega_{0m} \leq 0.281$ and $-1.123 \leq w_{0x} \leq -1.077$. All these results are fairly in agreement with those found with other model-independent or model-dependent parameterizations of the DE in the literature [46, 47, 48, 49, 50].

Finally, we integrate the scalar field equations of motion and reconstruct the interacting double quintessence potential using the best fit model parameters. We show that the reconstructed potential has a smooth dependence (i.e., without any discontinuity or multi-valuedness) on the scale factor a . We work out the approximate analytic expressions for the potential as function of the scalar fields, and find that they also exhibit the same smooth nature at early and late stages of the evolution of the universe.

This paper is organized as follows: in sec. 2 we describe the general framework of the multi-scalar (k-essence) DE scenario, following the formalism shown in refs. [42, 43] in the context of multi-field k-inflation. In sec. 3 we emphasize on a special case which involves two quintessence type of scalar fields with canonical kinetic terms in the Lagrangian, and with a specific kinetic interaction between the individual fields. Assuming suitable ansatze for the solutions of the field equations we work out the condition under which the cosmological constant barrier $w_x = -1$ could be crossed, and find the expression for the Hubble parameter maintaining this condition. In sec. 4 we fit our KIDQ model with the 307 Union SN Ia data [8], combined with the CMB+BAO results from WMAP and SDSS, to obtain the DE density and EoS profiles. In sec. 5 we use the best fit values of the model parameters to reconstruct phenomenologically the interacting double quintessence potential and determine the temporal variations of the scalar fields. We also work out the approximate analytic functional forms of the potential in terms of the scalar fields, at early and late stages of the evolution of the universe. In sec. 6, we conclude with a summary and some open questions. In the Appendix, we show how the KIDQ action, that we consider, could be derived from the two-field DBI action under certain approximations.

2. General Formalism

Let us consider the following action, in $(3+1)$ dimensions, for gravity minimally coupled with matter fields and N number of kinetically interacting (k-essence) scalar fields ϕ^I ($I = 1, \dots, N$):

$$S = \int d^4x \sqrt{-g} \left[\frac{R}{2\kappa^2} + \mathcal{L}_m + P(X^{IJ}, \phi^K) \right], \quad (1)$$

where $\kappa^2 = 8\pi G$ is the gravitational coupling constant, \mathcal{L}_m is the Lagrangian density for matter, that is considered to be pressureless dust. $P(X^{IJ}, \phi^K)$ is the multi-scalar Lagrangian density, with

$$X^{IJ} = -\frac{1}{2} g^{\mu\nu} \partial_\mu \phi^I \partial_\nu \phi^J, \quad (I, J = 1, \dots, N), \quad (2)$$

describing the kinetics of the scalar fields [42].

In a spatially flat Friedmann-Robertson-Walker (FRW) background, with line element

$$ds^2 = -dt^2 + a^2(t) [dr^2 + r^2 (d\vartheta^2 + \sin^2 \vartheta d\varphi^2)] \quad (3)$$

the above expression for X^{IJ} reduces to

$$X^{IJ} = X^{JI} = \frac{1}{2} \dot{\phi}^I \dot{\phi}^J = \frac{a^2 H^2}{2} \phi'^I \phi'^J, \quad (4)$$

where the dot denotes time derivative (d/dt) and the prime denotes derivative (d/da) with respect to the scale factor a , which has been normalized to unity at the present epoch $t = t_0$. $H \equiv \dot{a}/a$ is the Hubble parameter.

The Friedmann equations and the scalar field equations of motion are given by

$$H^2 \equiv \left(\frac{\dot{a}}{a} \right)^2 = \frac{\kappa^2}{3} (\rho_m + \rho_x) \quad , \quad \dot{H} \equiv \frac{\ddot{a}}{a} - \frac{\dot{a}^2}{a^2} = -\frac{\kappa^2}{2} [\rho_m + (\rho_x + p_x)] \quad , \quad (5)$$

$$\frac{d}{dt} \left(a^3 \frac{\partial P}{\partial X^{IJ}} \dot{\phi}^J \right) = a^3 \frac{\partial P}{\partial \phi^I}, \quad (6)$$

where ρ_m is the energy density of matter in the form pressureless dust, and ρ_x, p_x are the multi-field dark energy density and pressure, given respectively as

$$\rho_x = 2X^{IJ} \frac{\partial P}{\partial X^{IJ}} - P \quad , \quad p_x = P. \quad (7)$$

Assuming that there is no mutual interaction between matter and dark energy, the Friedmann equations (5) integrate to give $\rho_m = \rho_{0m} a^{-3}$, where ρ_{0m} is the matter density at the present epoch ($t = t_0, a = 1$). One also has the continuity equation for the dark energy

$$\dot{\rho}_x = -3H(\rho_x + p_x) \quad \Rightarrow \quad \rho'_x = -\frac{3}{a}(\rho_x + p_x). \quad (8)$$

From the Friedmann equations (5) one obtains the expressions for the DE EoS parameter w_x , the total EoS parameter w , and the deceleration parameter q :

$$w_x = \frac{p_x}{\rho_x} = -1 + \frac{2X^{IJ}}{\rho_x} \frac{\partial P}{\partial X^{IJ}}, \quad (9)$$

$$w = \frac{p_x}{\rho_m + \rho_x} = w_x \left(1 - \frac{\Omega_{0m}}{\tilde{H}^2 a^3} \right), \quad (10)$$

$$q \equiv -\frac{\ddot{a}}{aH^2} = \frac{1+3w}{2}, \quad (11)$$

where $\rho_{0c} = 3H_0^2/\kappa^2$ is the present critical density; H_0 being the value of H at the present epoch ($t = t_0$).

$$\tilde{H} \equiv \frac{H}{H_0} = \sqrt{\frac{\rho_x}{\rho_{0c}} + \frac{\Omega_{0m}}{a^3}}, \quad (12)$$

is the normalized Hubble parameter and $\Omega_{0m} = \rho_{0m}/\rho_{0c}$ is the present matter density parameter.

The transition from the decelerating regime to the accelerating regime takes place when the deceleration parameter q changes sign, i.e., the total EoS parameter w becomes less than $-1/3$, by Eq. (11), and the DE EoS parameter w_x is further less, by Eq. (10). The crossing from $w_x > -1$ to $w_x < -1$, on the other hand, requires a flip of sign of the quantity $X^{IJ}\partial P/\partial X^{IJ}$, presuming that the DE density ρ_x is positive definite. In the next section, we examine the plausibility of such a crossing by considering for simplicity a model involving only two fields ($N = 2$) with usual (canonical) kinetic terms (quintessence type), but with a specific type of kinetic interaction, which could have its origin in the two-field DBI action, as we show in the Appendix.

3. Kinetically interacting double quintessence

Let us take into account the following special form of the Lagrangian density for the DE, consisting of only two scalar fields:

$$P = \delta_{IJ}X^{IJ} - \gamma\sqrt{1 - \frac{\beta}{2}(\delta_{I,J-1} + \delta_{I-1,J})X^{IJ}} - V(\phi^I), \quad (13)$$

where β, γ are positive constants, $V(\phi^I)$ is the scalar potential, and the indices I, J run for 1, 2. Denoting the two fields as $\phi^I \equiv (\phi, \xi)$, we can re-write the above Lagrangian as

$$P = \frac{\dot{\phi}^2}{2} + \frac{\dot{\xi}^2}{2} - \gamma Q(\dot{\phi}, \dot{\xi}) - V(\phi, \xi), \quad \text{where } Q(\dot{\phi}, \dot{\xi}) = \sqrt{1 - \frac{\beta}{2}\dot{\phi}\dot{\xi}}. \quad (14)$$

This implies that the scalar fields ϕ and ξ have usual (canonical) kinetic energy densities (given respectively by the first two terms on the right hand side), and therefore are similar to ordinary quintessence fields. However they have a mutual kinetic interaction of a specific form proportional to $Q(\dot{\phi}, \dot{\xi})$, given above, which may originate from the two-scalar DBI action, approximated for $\beta \ll 1$ and $\gamma \gg 1$ (but $\gamma^{-1} \ll \beta$) as shown in the Appendix.

The dark energy pressure p_x is equal to P in Eq. (14), whereas the expression (7) for the dark energy density reduces to

$$\rho_x = \frac{\dot{\phi}^2}{2} + \frac{\dot{\xi}^2}{2} + \frac{\gamma}{Q(\dot{\phi}, \dot{\xi})} + V(\phi, \xi). \quad (15)$$

The DE equation of state parameter w_x , Eq. (9), now takes the form

$$w_x = \frac{p_x}{\rho_x} = -1 + \frac{1}{\rho_x} \left[\dot{\phi}^2 + \dot{\xi}^2 + \frac{\beta \gamma \dot{\phi} \dot{\xi}}{2Q(\dot{\phi}, \dot{\xi})} \right]. \quad (16)$$

The presumption that the parameter $\beta \ll 1$, is in support of the positivity of the term under the square root in the expression for $Q(\dot{\phi}, \dot{\xi})$ given in Eq. (14). That is, the requirement

$Q^2(\dot{\phi}, \dot{\xi}) > 0$ for the validity of the model, could be fulfilled when $\beta \ll 1$, even if $\dot{\phi}$ and $\dot{\xi}$ vary fairly rapidly with time and the product $\dot{\phi}\dot{\xi} > 0$. Considering further, $Q(\dot{\phi}, \dot{\xi})$ itself to be positive, the kinematical part of the DE density, given by the first three terms (kinetic energy densities of the fields plus their kinetic interaction) on the right hand side of Eq. (15), remains positive definite. As such, the total DE Hamiltonian is bounded from below and the model is quantum mechanically consistent. Moreover, since β, γ and $Q(\dot{\phi}, \dot{\xi})$ are all positive, it follows from Eq. (16) that, $w_x < -1$ (in some regime) necessarily implies the product $\dot{\phi}\dot{\xi} < 0$. In other words, the condition for the crossing of the $w_x = -1$ barrier at a particular epoch, is that one of the two fields (ϕ, ξ) must fall off with time, whereas the other one should increase with time.

Now, using Eqs. (15), (16) and the continuity equation (8), one obtains the following expression for the potential V as a function of the scale factor a :

$$V(a) = -\frac{\dot{\phi}^2(a) + \dot{\xi}^2(a)}{2} - \frac{\gamma}{Q(a)} + \Lambda - 3 \int^a \frac{d\tilde{a}}{\tilde{a}} \left[\dot{\phi}^2(\tilde{a}) + \dot{\xi}^2(\tilde{a}) + \frac{\beta\gamma \dot{\phi}(\tilde{a}) \dot{\xi}(\tilde{a})}{2 Q(\tilde{a})} \right], \quad (17)$$

where Λ is an integration constant. Plugging Eq. (17) back in Eq. (15) we get the DE density ρ_x as a function of a :

$$\rho_x(a) = \Lambda - 3 \int^a \frac{d\tilde{a}}{\tilde{a}} \left[\dot{\phi}^2(\tilde{a}) + \dot{\xi}^2(\tilde{a}) + \frac{\beta\gamma \dot{\phi}(\tilde{a}) \dot{\xi}(\tilde{a})}{2 Q(\tilde{a})} \right]. \quad (18)$$

One may note that Eq. (17) could also have been obtained by using the scalar field equations of motion (6), which in the present scenario reduce to

$$\begin{aligned} \frac{d}{dt} \left[a^3 \left(\dot{\phi} + \frac{\beta\gamma \dot{\xi}}{4Q(\dot{\phi}, \dot{\xi})} \right) \right] &= a^3 \frac{\partial V}{\partial \phi}, \\ \frac{d}{dt} \left[a^3 \left(\dot{\xi} + \frac{\beta\gamma \dot{\phi}}{4Q(\dot{\phi}, \dot{\xi})} \right) \right] &= a^3 \frac{\partial V}{\partial \xi}. \end{aligned} \quad (19)$$

Under a dimensional re-scaling:

$$\phi \leftrightarrow \frac{\phi}{\sqrt{\rho_{0c}}}, \quad \xi \leftrightarrow \frac{\xi}{\sqrt{\rho_{0c}}}, \quad \Lambda \leftrightarrow \frac{\Lambda}{\rho_{0c}}, \quad \beta \leftrightarrow \beta \rho_{0c}, \quad \gamma \leftrightarrow \frac{\gamma}{\rho_{0c}}, \quad (20)$$

the DE density, pressure, and the scalar potential change as

$$\rho_x \leftrightarrow \frac{\rho_x}{\rho_{0c}}, \quad p_x \leftrightarrow \frac{p_x}{\rho_{0c}}, \quad V \leftrightarrow \frac{V}{\rho_{0c}}, \quad (21)$$

while all the above equations (15) - (19) remain invariant. On the other hand, the expression (12) for the normalized Hubble parameter reduces to

$$\tilde{H}^2(a) = \rho_x(a) + \frac{\Omega_{0m}}{a^3} = \Lambda + \frac{\Omega_{0m}}{a^3} - 3 \int^a \frac{d\tilde{a}}{\tilde{a}} \left[\dot{\phi}^2(\tilde{a}) + \dot{\xi}^2(\tilde{a}) + \frac{\beta\gamma \dot{\phi}(\tilde{a}) \dot{\xi}(\tilde{a})}{2 Q(\tilde{a})} \right]. \quad (22)$$

Let us now consider the following ansatze for the kinetic energy densities of the scalar fields:

$$\begin{aligned} \rho_\phi^K(a) &= \frac{1}{2} \dot{\phi}^2(a) = \frac{1}{2} \left[f(a) + \sqrt{f^2(a) - k^2} \right], \\ \rho_\xi^K(a) &= \frac{1}{2} \dot{\xi}^2(a) = \frac{1}{2} \left[f(a) - \sqrt{f^2(a) - k^2} \right], \end{aligned} \quad (23)$$

where $f(a)$ is taken to be a positive definite and well-behaved function of a , k is a positive constant, and $f(a) > k$ at all epochs. Eqs. (23) imply that

$$\dot{\phi}^2 + \dot{\xi}^2 = 2f(a), \quad \text{and} \quad \dot{\phi}\dot{\xi} = \pm k. \quad (24)$$

We choose to take $\dot{\phi}\dot{\xi} = -k$, so that the DE EoS parameter w_x , Eq. (16), could be made less than -1 in some regime. Moreover, this choice guarantees the positivity of the square of the kinetic interaction, which now reduces to a constant:

$$Q^2 = 1 + \frac{\beta k}{2}. \quad (25)$$

The expressions for the time derivatives of the scalar fields are given by

$$\dot{\phi}(a) = \frac{\sqrt{f(a) - k} + \sqrt{f(a) + k}}{\sqrt{2}}, \quad \dot{\xi}(a) = \frac{\sqrt{f(a) - k} - \sqrt{f(a) + k}}{\sqrt{2}}, \quad (26)$$

whereas from Eqs. (16), (18) and (17), we respectively obtain the following expressions for the DE EoS parameter and density, and the scalar potential:

$$w_x(a) = -1 + \frac{1}{\rho_x(a)} \left[2f(a) - \frac{\beta\gamma k}{2Q} \right], \quad (27)$$

$$\rho_x(a) = \Lambda + \frac{3\beta\gamma k}{2Q} \ln a - 6 \int^a \frac{f(\tilde{a})}{\tilde{a}} d\tilde{a}, \quad (28)$$

$$V(a) = \Lambda + \frac{3\beta\gamma k}{2Q} \ln a - f(a) - \frac{\gamma}{Q} - 6 \int^a \frac{f(\tilde{a})}{\tilde{a}} d\tilde{a}. \quad (29)$$

Let us now assume a specific form of the function $f(a)$, given by

$$f(a) = Aa^{-\nu} + k, \quad \text{where} \quad A > 0, \quad 0 < \nu < 3, \quad (30)$$

so that the criterion $f(a) > k > 0$ is automatically satisfied. Furthermore, $0 < \nu < 3$ ensures that $f(a)$, and hence the kinetic energy densities $\frac{1}{2}\dot{\phi}^2$ and $\frac{1}{2}\dot{\xi}^2$ of the scalar fields, fall off with increasing values of the scale factor a . However, these fall offs are not faster than that of the matter density ($\rho_m \sim 1/a^3$). This is essential in order that the quantities $\frac{1}{2}\dot{\phi}^2$ and $\frac{1}{2}\dot{\xi}^2$, which compose the total DE density ρ_x , come to dominate ρ_m at late times, i.e., for large values of a .

Eqs. (26) reduce to

$$\dot{\phi}(a) = \frac{\sqrt{Aa^{-\nu}} + \sqrt{Aa^{-\nu} + k}}{\sqrt{2}}, \quad \dot{\xi}(a) = \frac{\sqrt{Aa^{-\nu}} - \sqrt{Aa^{-\nu} + k}}{\sqrt{2}}, \quad (31)$$

and the Eqs. (27) - (29), for w_x, ρ_x and V , take the form

$$w_x(a) = -1 + \frac{2}{\rho_x(a)} (Aa^{-\nu} - B), \quad (32)$$

$$\rho_x(a) = \frac{6A}{\nu} a^{-\nu} + 6B \ln a + \Lambda, \quad (33)$$

$$V(a) = V_0 + \left(\frac{6}{\nu} - 1 \right) A (a^{-\nu} - 1) + 6B \ln a, \quad (34)$$

where we have defined

$$B = k \left(\frac{\beta\gamma}{4Q} - 1 \right) = \text{constant}, \quad (35)$$

and V_0 is the value of the scalar potential V at the present epoch ($t = t_0, a = 1$):

$$V_0 = \left(\frac{6}{\nu} - 1\right) A + \left(\Lambda - k - \frac{\gamma}{Q}\right). \quad (36)$$

From Eqs. (22) and (33) one also obtains the following expression for the normalized Hubble rate $\tilde{H} = H/H_0$:

$$\tilde{H}^2(a) = \frac{6A}{\nu a^\nu} + \frac{\Omega_{0m}}{a^3} + 6B \ln a + \Lambda. \quad (37)$$

At $a = 1$ (present epoch), $\tilde{H} = 1$, whence

$$\Lambda = 1 - \Omega_{0m} - \frac{6A}{\nu}, \quad (38)$$

and the above expression (37) reduces to

$$\tilde{H}^2(a) = 1 + \frac{6A}{\nu a^\nu} (1 - a^\nu) + \frac{\Omega_{0m}}{a^3} (1 - a^3) + 6B \ln a. \quad (39)$$

In the next section, we fit this Eq. (39) with the latest Supernova Ia data [8], as well as with the CMB+BAO results from WMAP and SDSS [14, 15], and determine the DE density and EoS profiles over the red-shift range that is probed.

4. Observational constraints

We perform a χ^2 analysis so as to constrain the model parameters A, B and Ω_{0m} , for two specific choices of the index ν ($= 1, 2$) in the ansatz (30). The SN Ia Union data-set [8], which we use, consists of 307 most reliable data points that range up to red-shift $z = (1/a - 1) \sim 1.7$, and include large samples of SN Ia from older data-sets [1, 2, 3, 4], high- z Hubble Space Telescope (HST) observations and the SN Legacy Survey (SNLS) [5].

The SN Ia data provide the observed distance modulus $\mu_{obs}(z_i)$, with the respective 1σ uncertainty $\sigma_i(z_i)$, for SN Ia located at various red-shifts z_i , ($i = 1, \dots, 307$). The χ^2 for the SN observations is, on the other hand, expressed as

$$\chi_{SN}^2(\mu_0; \Omega_{0m}, A, B) = \sum_{i=1}^{307} \frac{[\mu_{obs}(z_i) - \mu(z_i)]^2}{\sigma_i^2(z_i)}, \quad (40)$$

where

$$\mu(z_i) = 5 \log_{10} [D_L(z_i)] + \mu_0, \quad (41)$$

is the theoretical distance modulus.

$$D_L(z_i) = (1 + z_i) \int_0^{z_i} \frac{d\tilde{z}_i}{\tilde{H}(\tilde{z}_i; \Omega_{0m}, A, B)}, \quad (42)$$

is the Hubble free luminosity distance in terms of the parameters (Ω_{0m}, A, B) , and

$$\mu_0 = 5 \log_{10} \left[\frac{H_0^{-1}}{Mpc} \right] + 25 = 42.38 - 5 \log_{10} h, \quad (43)$$

h being the Hubble constant H_0 in units of $100 \text{ Km s}^{-1} \text{ Mpc}^{-1}$. The parameter μ_0 is a nuisance parameter, independent of the data points, and has to be uniformly marginalized over (i.e.,

integrated out). For such a marginalization one may follow the procedure shown in refs. [32, 51, 52], where χ_{SN}^2 is first expanded suitably in terms of μ_0 . Then one finds the value of μ_0 for which such an expanded form of χ_{SN}^2 is minimum. Substituting this value of μ_0 back in χ_{SN}^2 , finally enables one to perform the minimization of the resulting expression with respect to the parameters (Ω_{0m}, A, B) , in order to determine the values of the latter best fit with the SN Ia observations.

The CMB shift parameter \mathcal{R} , that relates the angular diameter distance to the last scattering surface (at red-shift z_{ls}) with the co-moving sound horizon scale at recombination and the angular scale of the first acoustic peak in the CMB temperature fluctuations power spectrum [15, 53], is given by

$$\mathcal{R}(z_*) = \Omega_{0m}^{1/2} \int_0^{z_*} \frac{d\tilde{z}}{\tilde{H}(\tilde{z}; \Omega_{0m}, A, B)}, \quad (44)$$

where z_* is the red-shift of recombination. The WMAP five year data [14] updates $z_* = 1090.04 \pm 0.93$ and the observed shift parameter $\mathcal{R}_{obs}(z_*) = 1.710 \pm 0.019$. The χ^2 for the CMB observations is given by

$$\chi_{CMB}^2 = \frac{(\mathcal{R}_{obs} - \mathcal{R})^2}{\sigma_R^2}, \quad (45)$$

where σ_R is the 1σ error in the WMAP data [14].

Now, the scalar spectral index n_s , which determines the observed value of the BAO peak distance parameter \mathcal{A}_{obs} from the distribution of the SDSS luminous red galaxies [15] through the relation $\mathcal{A}_{obs} = 0.469 (n_s/0.98)^{-0.35} \pm 0.017$, is updated by the WMAP five year data as $n_s = 0.960 \pm 0.013$ (see the first ref. of [14], see also ref. [52]). The theoretical expression for the distance parameter is, on the other hand, given by

$$\mathcal{A} = \Omega_{0m}^{1/2} \left[\frac{1}{z_b \sqrt{\tilde{H}(z_b)}} \int_0^{z_b} \frac{d\tilde{z}}{\tilde{H}(\tilde{z}; \Omega_{0m}, A, B)} \right]^{2/3}, \quad (46)$$

where $z_b = 0.35$. The χ^2 for the BAO observations is expressed as

$$\chi_{BAO}^2 = \frac{(\mathcal{A}_{obs} - \mathcal{A})^2}{\sigma_A^2}, \quad (47)$$

σ_A being the 1σ error in the SDSS data [15].

The total χ^2 , which needs to be minimized in order to determine the likelihood of the model parameters (Ω_{0m}, A, B) with the entire SN+CMB+BAO data, is thus given as

$$\chi_{total}^2 = \chi_{SN}^2 + \chi_{CMB}^2 + \chi_{BAO}^2. \quad (48)$$

Of course, χ_{SN}^2 has already been minimized with respect to the nuisance parameter μ_0 , Eq. (43), by the process discussed above.

For two specific choices of the index ν ($= 1, 2$), that appears in the ansatz (30), the best fit values the parameters (Ω_{0m}, A, B) , as well as the minimized value of χ_{total}^2 , are shown in the table 1. Fig. 1 shows the evolution of $w_x(z)$ and $\rho_x(z)$ (alongwith the corresponding 1σ errors) throughout the entire red-shift range $0 \leq z \leq 1.75$ of the available data, for both the choices

Index ν	Best fit model parameters			Minimized χ^2_{total}
	Ω_{0m}	A	B	
1	0.2790	0.2062	0.2506	311.07
2	0.2816	0.0505	0.0782	311.27

Table 1. Values of the parameters (Ω_{0m}, A, B) of the model, best fit with SN+CMB+BAO observations, and the minimized total χ^2 , for the choices $\nu = 1, 2$.

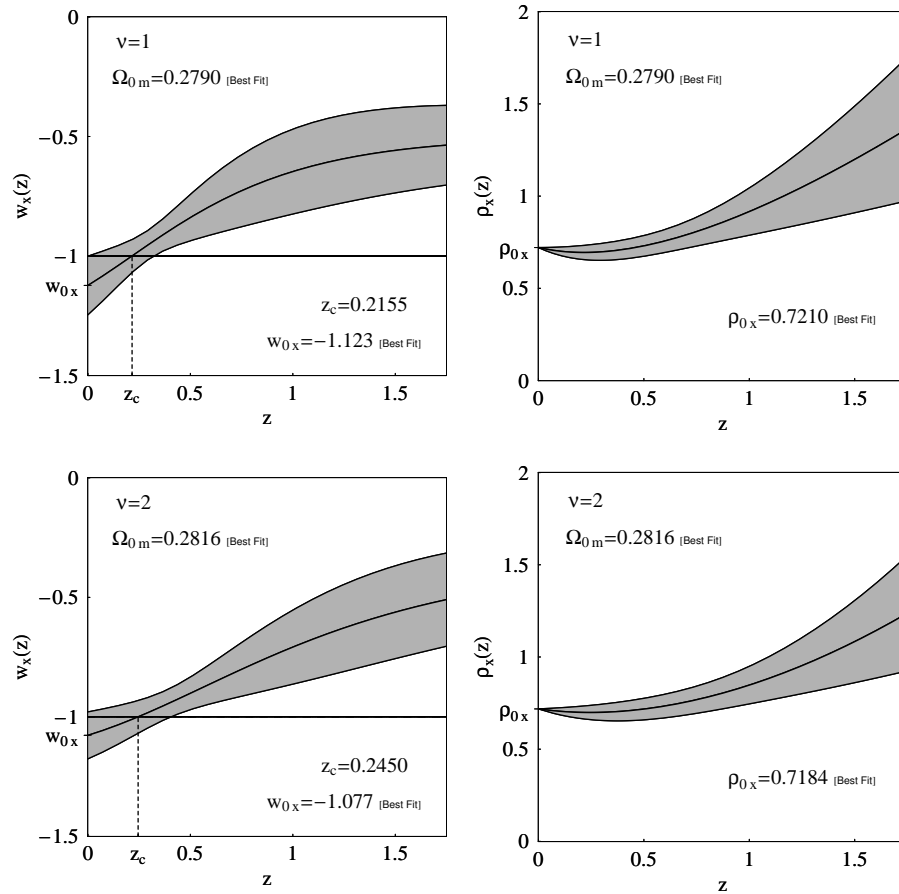


Figure 1. Evolution of $w_X(z)$ and $\rho_X(z)$ (best fit with the SN+CMB+BAO observations) throughout the red-shift range $0 \leq z \leq 1.75$ alongwith the corresponding 1σ error (shaded) regions, are shown for the choices $\nu = 1$ (upper panels) and $\nu = 2$ (lower panels). The point z_c denotes the red-shift at which the $w_X = -1$ line is crossed, and w_{0X}, ρ_{0X} are respectively the values of w_X, ρ_X at the present epoch ($z = 0$).

of ν . The maximum likelihood of the present value w_{0X} of the DE EoS parameter is found to be -1.123 for $\nu = 1$ and -1.077 for $\nu = 2$. Both these values are well within the limits, viz.,

$-1.33 \leq w_{0X} \leq 0.79$, obtained in model-independent estimates with the SN+CMB+BAO data in ref. [14]. On the other hand, the red-shift $z = z_c$ at which the best fit w_X makes a transition from a value > -1 to a value < -1 is found to be 0.2155 for $\nu = 1$ and 0.2450 for $\nu = 2$. However, w_X stays well below zero even for $z = 1.75$, implying that DE is varying slowly with red-shift. The above values of z_c also agree fairly well with other independent studies [50]. The best fit DE density at the present epoch, ρ_{0X} , is found to be equal to 0.7210 for $\nu = 1$ and 0.7184 for $\nu = 2$. Remembering the dimensional re-scaling of the DE density, viz., $\rho_X \leftrightarrow \rho_X/\rho_{0c}$, that we have performed earlier in Eq. (21), one may note that the ρ_{0X} shown in Fig. 1 is identical with the present DE density parameter $\Omega_{0X} = \rho_{0X}/\rho_{0c}$ (by virtue of the dimensional re-scaling). In other words, since the DE density ρ_X is effectively measured in units of the present critical density ρ_{0c} , one has $\rho_{0X} \equiv \Omega_{0X}$. It may also be noted that the sum of the best fit Ω_{0m} and the best fit Ω_{0X} is exactly equal to 1 (for both $\nu = 1$ and $\nu = 2$), as it should be in accord with our prior assumption of the spatial flatness of the metric. This therefore proves the correctness of the χ^2 -fitting of the model with the observational data.

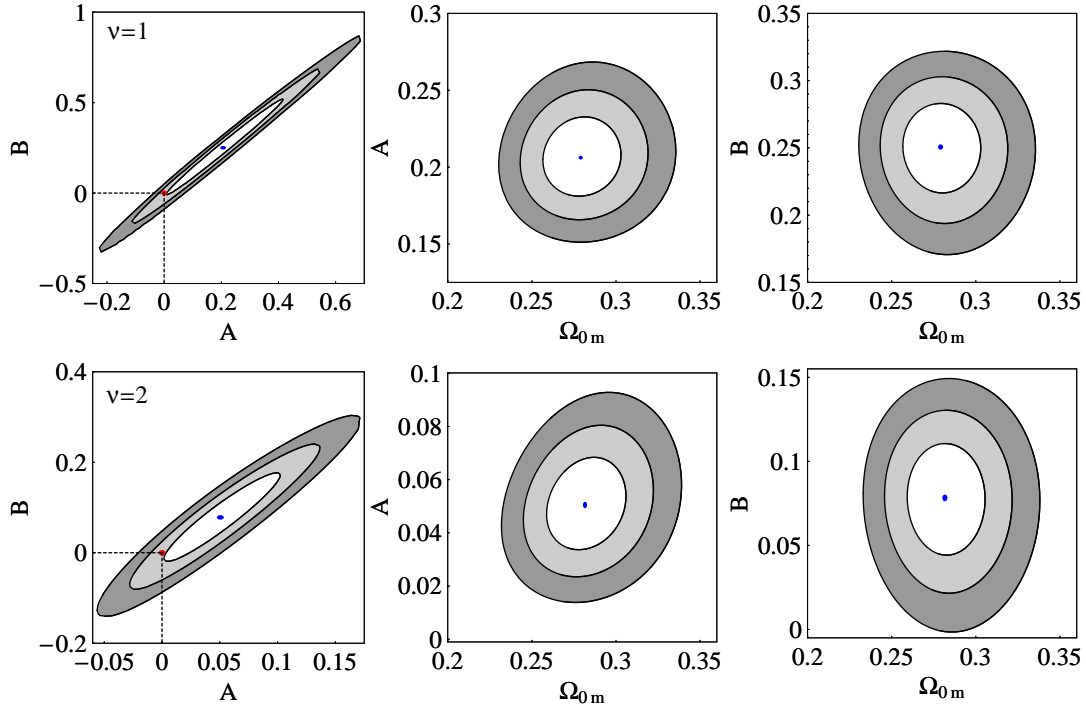


Figure 2. 1σ , 2σ and 3σ contours in the parameter spaces $A - B$ (for best fit Ω_{0m}), $\Omega_{0m} - A$ (for best fit B), and $\Omega_{0m} - B$ (for best fit A), are shown for the choices $\nu = 1$ (upper panels) and $\nu = 2$ (lower panels). The best fit points for both the choices are shown by the dots at the middle of all the 1σ contours, whereas the cosmological constant, which corresponds to $A = B = 0$, is shown by the dot that is found to lie on edge of the 1σ $A - B$ contour for both the choices (left panels, upper and lower).

The 1σ , 2σ and 3σ contour plots of (i) A versus B (with Ω_{0m} fixed at its best fit value), (ii) Ω_{0m} versus A (with best fit B), and (iii) Ω_{0m} versus B (with best fit A), are shown in Fig.

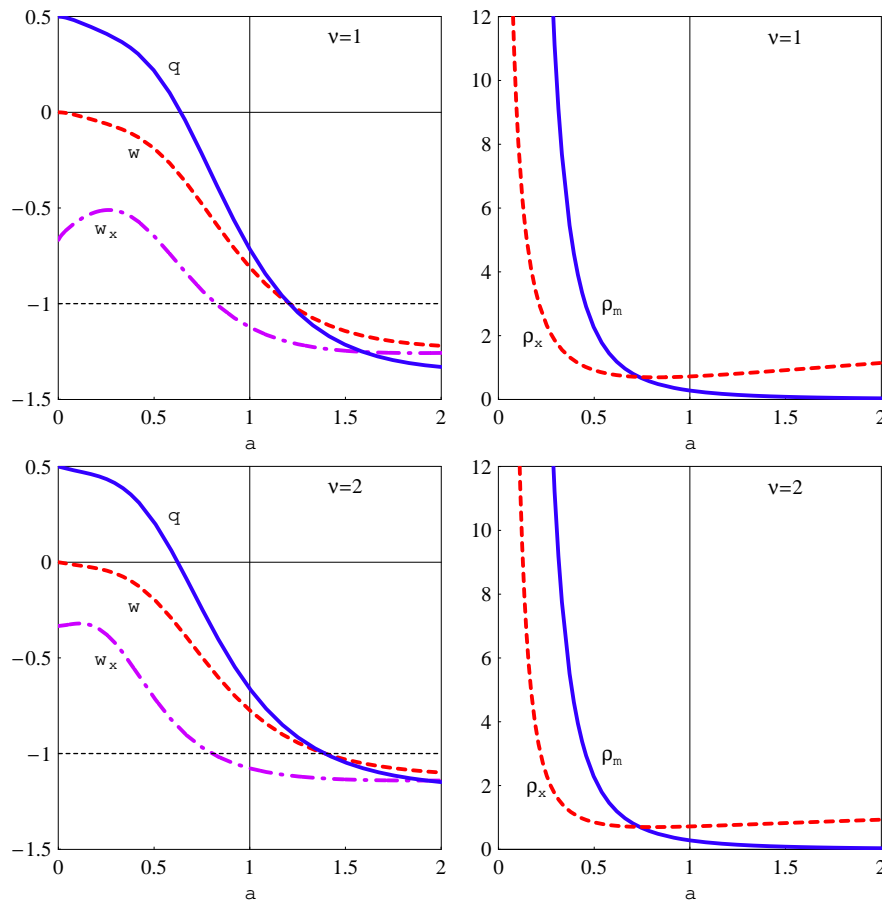


Figure 3. Left panels: extrapolations of w_x , w and q (best fit with SN+CMB+BAO data), as functions of the scale factor a , to the range $0 \leq a \leq 2$, for the choices $\nu = 1$ (upper left) and $\nu = 2$ (lower left). Right panels: extrapolated variations of ρ_x and ρ_m (best fit with SN+CMB+BAO data) with the scale factor a , to the range $0 \leq a \leq 2$, for $\nu = 1$ (upper right) and $\nu = 2$ (lower right). The $a = 1$ line denotes the present epoch. The transition from a decelerating regime to an accelerating regime (i.e., the change of sign of q) takes place at $a \sim 0.64$. The dark energy density ρ_x is found to nearly follow the matter density ρ_m for a considerable period in the past until becoming dominant very recently, and increases slowly in the future.

2, for the choices $\nu = 1$ (upper panels) and $\nu = 2$ (lower panels). The case $A = B = 0$, which resembles a cosmological constant DE, is found to be about 1σ away from the best fit point in the A versus B contours (left panels), for both the choices.

The upper and lower left panels of Fig. 3 depict the variations of the best fit DE EoS parameter $w_x(a)$, as well as the total EoS parameter $w(a)$, Eq. (10), and the deceleration parameter $q(a)$, Eq. (11), obtained as functions of the scale factor a (using the best fit values of the parameters Ω_{0m}, A, B) and extrapolated to the range $0 \leq a \leq 2$, for the choices $\nu = 1$ and $\nu = 2$ respectively. The range covers all of the past, i.e., right from the big bang ($a = 0, z = \infty$) to the present ($a = 1, z = 0$), and a considerable part in the future, up to $a = 2$ ($z = -1/2$), i.e.,

when the present size of the universe gets doubled. Both w_x and w are negative in the past and tend to become constant at a value close to each other and a little less than -1 in the future. The value of q , on the other hand, changes from positive to negative, i.e., the transition from deceleration to acceleration takes place at $a = 0.640$ ($z = 0.562$) for $\nu = 1$ and at $a = 0.624$ ($z = 0.603$) for $\nu = 2$. In the future, q also remains negative and tends to be steady at a value close to w and w_x . Thus the accelerated regime $q < 0$, as well as the ‘super-acceleration’ ($w_x < -1$), do not appear to be transient in the present model.

The variations of the extrapolated best fit DE density ρ_x and the matter density ρ_m , with the scale factor a in the range $0 \leq a \leq 2$, are shown respectively for the choices $\nu = 1$ and $\nu = 2$, in upper and lower right panels of Fig. 3. For a considerable period in the past the DE density nearly follows the track of the matter density, until exceeding the latter at scale factor $a \simeq 0.75$, and dominant thereafter. In other words, ρ_x decreases with a in a similar manner as ρ_m does in the early regimes, until at a recent epoch $a \simeq 0.75$, when the DE begins to dominate. This behaviour, although not distinctly similar to that due to the tracker quintessence fields [18], may perhaps stand as a possible resolution to the coincidence problem [54]. One can, in fact, trace the similarity of the early universe profiles of ρ_x and ρ_m to the form of the chosen ansatz (30) for the field solutions and the resulting expression (33) for ρ_x . In the early epochs, i.e., for small values of a , the DE density ρ_x in Eq. (33) is dominated by the inverse power-law term $\sim Aa^{-\nu}$, similar to the matter density $\rho_m = \Omega_{0m}a^{-3}$. However, since $\nu < 3$ and the best fit value of A is of the order of the best fit Ω_{0m} , ρ_x is smaller than ρ_m , and decreases less rapidly than the latter, for sufficiently smaller values of a . As a increases, the value of ρ_x eventually exceeds ρ_m due to the presence of the positive constant term ($= \Lambda$, given by Eq. (38)) in the expression (33) for ρ_x . The $B \ln a$ term in Eq. (33), which is negative for $a < 1$ (i.e., past), is on the other hand, rather sub-dominant compared to Λ and does not play a very significant role either in the past or in near future. This is the reason why, the DE density ρ_x increases slowly and does not shoot up to very high values even at a scale factor as large as $a = 2$, giving rise to singularities in finite future. Admittedly, of course $\rho_x \rightarrow \infty$ as $a \rightarrow \infty$ due to the presence of the logarithmic term in ρ_x . Thus, the extrapolations of the cosmological quantities using the best fit values of the model parameters, obtained in the red-shift range $0 \leq z \leq 1.75$, appear to hold for very distant past and future.

In what follows, we integrate the expressions (31) numerically in the next section and use the values of Ω_{0m} , A and B best fit with the data, so as to determine the variations of the scalar fields ϕ and ξ with the scale factor a . We also reconstruct the potential V , given in Eq. (34), as a function of a , using these values of the parameters (Ω_{0m} , A , B), and finally, we work out the approximate analytic expressions for the functional variation of V with ϕ and ξ , in the regimes $a \ll 1$ (distant past) and $a \lesssim 1$ (recent past).

5. Reconstruction of the scalar potential

Let us recall Eqs. (31), from which one can derive the following equations for the derivatives of the scalar fields ϕ and ξ with respect to the scale factor a :

$$H_0 \phi'(a) = \frac{\sqrt{Aa^{-\nu}} + \sqrt{Aa^{-\nu} + k}}{\sqrt{2} a \tilde{H}(a)}, \quad H_0 \xi'(a) = \frac{\sqrt{Aa^{-\nu}} - \sqrt{Aa^{-\nu} + k}}{\sqrt{2} a \tilde{H}(a)}, \quad (49)$$

where $\tilde{H}(a)$ is as given by Eq. (37) or (39), in terms of the model parameters (Ω_{0m}, A, B) .

Assuming the initial condition that $\phi = \xi = 0$ at $a = 0$, one may re-write the above equations in integral form as

$$H_0 \phi(a) = \sqrt{\frac{A}{2}} [I_+(a) - I_+(0)], \quad H_0 \xi(a) = \sqrt{\frac{A}{2}} [I_-(a) - I_-(0)], \quad (50)$$

where

$$I_{\pm}(a) = \int^a \frac{d\tilde{a}}{\tilde{a}^{(1+\nu/2)} \tilde{H}(\tilde{a})} \left[1 \pm \sqrt{1 + \frac{2k\tilde{a}^\nu}{A}} \right]. \quad (51)$$

Again, denoting $\phi = \phi_0$ and $\xi = \xi_0$ at the present epoch ($a = 1$), we have

$$H_0 \phi_0 = \sqrt{\frac{A}{2}} [I_+(1) - I_+(0)], \quad H_0 \xi_0 = \sqrt{\frac{A}{2}} [I_-(1) - I_-(0)]. \quad (52)$$

From Eqs. (50) and (52), one therefore finds

$$\frac{\phi(a)}{\phi_0} = \frac{I_+(a) - I_+(0)}{I_+(1) - I_+(0)}, \quad \frac{\xi(a)}{\xi_0} = \frac{I_-(a) - I_-(0)}{I_-(1) - I_-(0)}. \quad (53)$$

Now, in order to perform the integrations in I_{\pm} , Eq. (51), one has to assign a particular value to the parameter k . Eliminating k from Eqs. (25) and (35) we find that the kinetic interaction Q satisfies the following cubic equation involving the parameters β, γ and B :

$$4Q^3 - \beta\gamma Q^2 + 2(\beta B - 2)Q + \beta\gamma = 0. \quad (54)$$

Solving this equation and substituting the feasible root^{||} back in the relation (25), one finds k in terms of β, γ and B only. For B , we use its values best fit with the observational data, given in table 1 for the choices $\nu = 1$ and $\nu = 2$. For β and γ , we recall that their values should be such that the condition $\gamma^{-1} \ll \beta \ll 1$ is satisfied and the KIDQ Lagrangian (14) could emerge as an approximation to the two-field DBI Lagrangian (see the Appendix). Henceforth, assuming typically $\beta = 0.01$ and $\gamma = 10^4$, we find $k = 0.012$ for $\nu = 1$ and $k = 0.004$ for $\nu = 2$. Also, using the best fit values of the parameters Ω_{0m}, A and B , on which \tilde{H} depends, and performing numerically the integrations in I_{\pm} , Eq. (51), we finally determine the variations of the normalized scalar fields ϕ/ϕ_0 and ξ/ξ_0 with the scale factor a , for $\nu = 1$ and $\nu = 2$. Similarly, we also find how the quantity $V - V_0$, given by Eq. (34), varies with a , for the same choices of ν . Such variations, extrapolated to the range $0 \leq a \leq 2$, are shown in Fig. 4. We observe that both ϕ/ϕ_0 and ξ/ξ_0 increases with increasing a , however ξ/ξ_0 grows much faster than ϕ/ϕ_0 , whose variation gradually decreases with a (see the left panels of Fig 4). As such

^{||} Feasibility here implies that one should pick only that root Q which is real and greater than unity, so that the presumption of the positivity of k is ensured through the relation (25).

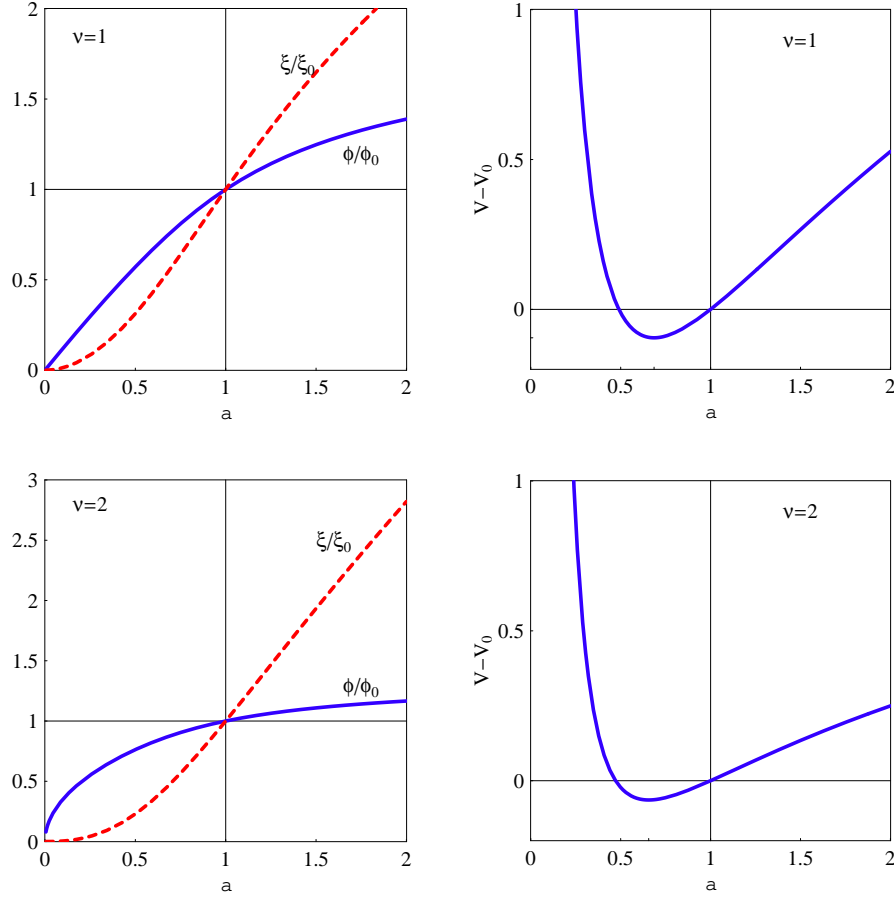


Figure 4. Evolutions of the normalized scalar fields ϕ/ϕ_0 and ξ/ξ_0 (left panels), and the scalar potential V minus its present value V_0 (right panels), with the scale factor a , for the choices $\nu = 1$ and $\nu = 2$. Such evolutions, which are reconstructed using the best fit values of the model parameters Ω_{0m} , A and B , have been extrapolated to the range $0 \leq a \leq 2$. The vertical line $a = 1$ resembles the present epoch.

the ratio ξ/ξ_0 , which has been less than ϕ/ϕ_0 in the past (i.e., $a < 1$), becomes greater than ϕ/ϕ_0 for $a > 1$ and grows to high values as we extrapolate it to far future. The potential V , on the other hand, decreases from a very high value ($\gg V_0$, its present value) in the early epochs, reaches a minimum ($< V_0$) at some point $a = a_m$ in the past, and increases steadily thereafter. However, the entire profile of $V - V_0$ for both $\nu = 1$ and $\nu = 2$ (shown in the right panels of Fig 4), is not symmetric about the minimum value $V_m - V_0$. In fact, the asymmetry is more when $\nu = 2$, rather than when $\nu = 1$. That is, the potential, after reaching its minimum, increases rather slowly for greater values of ν . The values of a_m and V_m (not shown in Fig. 4) could be calculated by extremizing the expression (34) for V :

$$a_m = \left[\frac{(6 - \nu) A}{6 B} \right]^{1/\nu}, \quad V_m = V_0 - \frac{(6 - \nu) A}{\nu} + \frac{6 B}{\nu} \ln \left[\frac{(6 - \nu) A}{6 B} \right]. \quad (55)$$

For $\nu = 1$, $a_m = 0.6856$ and $V_m - V_0 = -0.0948$, whereas for $\nu = 2$, $a_m = 0.6558$ and $V_m - V_0 = -0.0643$. Therefore, the greater the value of ν , the earlier is the occurrence of the minimum in the past, and the lesser is its value in magnitude.

The overall variation of the potential V with the scale factor a could be explained as follows: In the very early epochs $V - V_0$, given by Eq. (34), is very large and positive due to the dominance of the positive inverse power-law term $(6/\nu - 1)Aa^{-\nu}$. With the increase of a , this term rapidly diminishes, and $V - V_0$ becomes negative when the term $6B \ln a$, which is negative for $a < 1$ (past), starts to dominate over the positive second term on the right hand side of Eq. (34). Eventually, $V - V_0$ reaches the minimum, and then the potential V starts to increase as the term $6B \ln a$, though negative, gradually decreases in magnitude. V becomes equal to V_0 at the present epoch ($a = 1$) and after that $V - V_0$ increases with positive values as the logarithmic term becomes positive and increases with a . The asymmetry of the two sides of the minimum is obvious, because one is due to a power-law fall off and the other is due to a logarithmic increment. Also, for a bigger value of ν (here $\nu = 2$), the power-law fall off is faster. The asymmetry is therefore more distinct, the minimum is attained earlier, and the minimum value V_m is smaller in magnitude.

To reconstruct the potential V as a function of the fields ϕ and ξ , we need to solve the Eqs. (49) (or, equivalently need to work out the integrals I_{\pm} , Eq. (51)) analytically. However, this is very difficult because of the fairly complicated form of the normalized Hubble parameter \tilde{H} , given by Eq. (39). As an alternative, we resort to the following two regimes which are relevant for us: (i) $a \ll 1$ (early past) and (ii) $a \simeq 1$ (recent past, present, and near future), and work out the approximate functional form of $V(\phi, \xi)$ in these regimes.

(i) Early Universe:

For $a \ll 1$, the Hubble expansion is dominated by the inverse power-law terms in Eq. (37). As such, one can approximate:

$$\tilde{H}^2(a) \approx \frac{6A}{\nu a^\nu} + \frac{\Omega_{0m}}{a^3}. \quad (56)$$

Now, from Eqs. (50) and (51), we have

$$H_0 [\phi(a) + \xi(a)] = \sqrt{2A} [I(a) - I(0)], \quad (57)$$

where

$$I(a) = \frac{1}{2} [I_+(a) + I_-(a)] = \int^a \frac{d\tilde{a}}{\tilde{a}^{1+\nu/2} \tilde{H}(\tilde{a})}. \quad (58)$$

Using the approximated form (56) of \tilde{H} , we get

$$I(a) \approx \frac{1}{3-\nu} \sqrt{\frac{2\nu}{3A}} \sinh^{-1} \left(\sqrt{\frac{6A}{\nu\Omega_{0m}}} a^{(3-\nu)/2} \right) \Rightarrow I(0) \approx 0, \quad (59)$$

whence

$$H_0 [\phi(a) + \xi(a)] \approx \frac{2}{3-\nu} \sqrt{\frac{\nu}{3}} \sinh^{-1} \left(\sqrt{\frac{6A}{\nu\Omega_{0m}}} a^{(3-\nu)/2} \right). \quad (60)$$

Inverting this relation and substituting in Eq. (34), one finally obtains

$$\begin{aligned}
 V(\phi, \xi) \approx & V_0 + \left(\frac{6}{\nu} - 1 \right) A \left(\frac{\nu \Omega_{0m}}{6A} \right)^{-\nu/(3-\nu)} \sinh^{-2\nu/(3-\nu)} \left[\frac{3-\nu}{2} \sqrt{\frac{3}{\nu}} H_0 \cdot (\phi + \xi) \right] \\
 & + \frac{12B}{3-\nu} \ln \left\{ \sinh \left[\frac{3-\nu}{2} \sqrt{\frac{3}{\nu}} H_0 \cdot (\phi + \xi) \right] \right\} \\
 & - \left(\frac{6}{\nu} - 1 \right) A + \frac{6B}{3-\nu} \ln \left(\frac{\nu \Omega_{0m}}{6A} \right).
 \end{aligned} \tag{61}$$

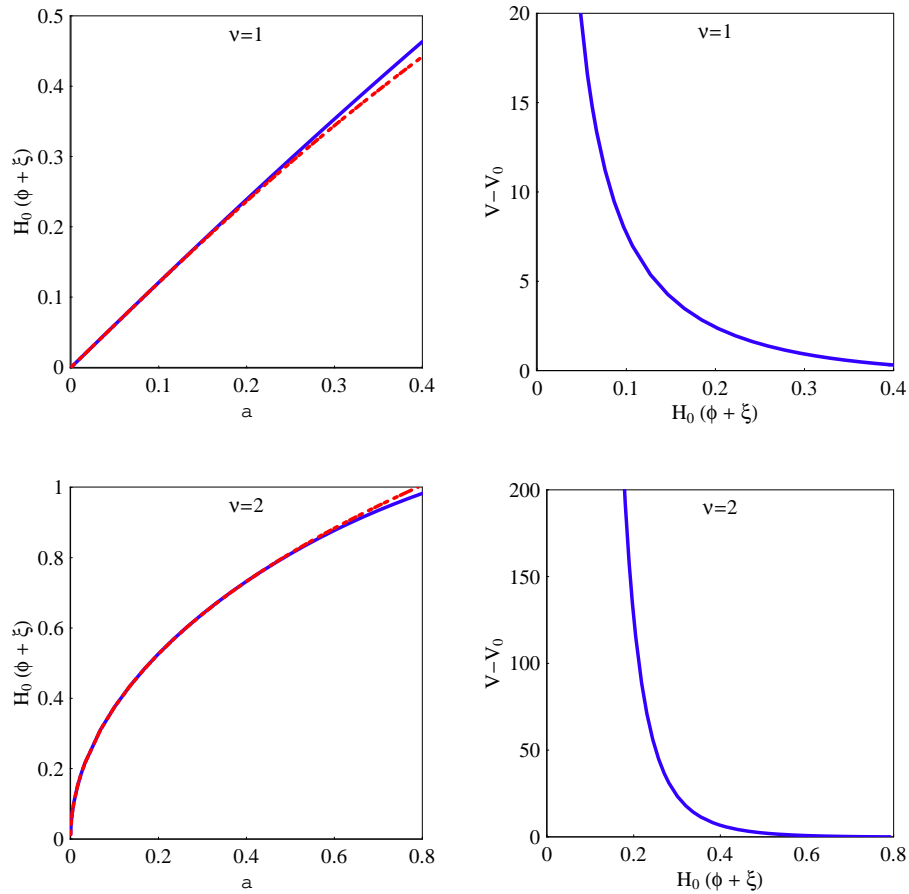


Figure 5. Exact (solid line) and approximated (dashed line) variations of the quantity $H_0(\phi + \xi)$ with the scale factor a in the early epochs ($a \ll 1$), for the choices $\nu = 1$ (upper left) and $\nu = 2$ (lower left). The approximation is found to hold up to $a \sim 0.3$ for $\nu = 1$, and up to $a \sim 0.7$ for $\nu = 2$. The right panels show the variation of the approximated $V - V_0$ with $H_0(\phi + \xi)$ for the range of validity of the approximation, in the cases $\nu = 1$ and $\nu = 2$ (upper right and lower right, respectively).

The left panels of Fig. 5 show how the approximated form of the quantity $H_0(\phi + \xi)$, as well as its exact form (obtained by working out the integral I , Eq. (58), numerically), vary with the scale factor a , for the choices $\nu = 1$ (upper left) and $\nu = 2$ (lower left). Whereas for $\nu = 1$,

the approximation is found to be valid only up to $a \sim 0.3$, it holds good till $a \sim 0.7$ for $\nu = 2$. Within the region of validity of the approximation, $H_0(\phi + \xi)$ increases almost linearly with a for $\nu = 1$, whereas for $\nu = 2$, $H_0(\phi + \xi)$ increases but gradually slows down as a increases. The variation of the approximated $V - V_0$ as a function of the fields ϕ and ξ , Eq. (61), is shown for $\nu = 1$ and $\nu = 2$ in the upper right and lower right panels of Fig. 5 respectively. Both these plots extend up to the range of a for which the approximation is valid in respective cases. The potential varies smoothly (i.e, without any discontinuity or multi valued-ness) with $H_0(\phi + \xi)$, as with the scale factor a (in Fig. 4). Also since $H_0(\phi + \xi)$ increases monotonically with a , the nature of the $V - V_0$ versus $H_0(\phi + \xi)$ plots in Fig. 5 is similar to the nature of the $V - V_0$ versus a plots in Fig. 4 for smaller values of a .

(ii) Recent Universe:

Expanding the expression (39) for \tilde{H} in powers of $(1 - a)$, for $a \approx 1$ (i.e., close to the present epoch), and retaining only the terms linear in $(1 - a)$ we have

$$\tilde{H}^2(a) \approx 1 + \tilde{h}(1 - a), \quad \text{where} \quad \tilde{h} = 6 \left(A - B + \frac{\Omega_{0m}}{2} \right), \quad (62)$$

for both $\nu = 1$ and $\nu = 2$. Now, from Eqs. (50), (51) and (52), one obtains¶

$$H_0 [(\phi(a) - \phi_0) + (\xi(a) - \xi_0)] = \sqrt{2A} [I(a) - I(1)], \quad (63)$$

where $I(a)$ is the integral given by Eq. (58). One can evaluate $I(a)$ numerically for the choices $\nu = 1$ and $\nu = 2$ and find $H_0 [(\phi - \phi_0) + (\xi - \xi_0)]$, using the best values of the parameters Ω_{0m} , A and B . However, to determine the functional form $V(\phi, \xi)$, we need to work out the integral $I(a)$ analytically. Let us separately consider the cases $\nu = 1$ and $\nu = 2$ as follows:

For $\nu = 1$: The expression (34) for the potential V can be approximated as

$$V(a) = V_0 + (5A - 6B)(1 - a). \quad (64)$$

On the other hand, the approximate analytic evaluation of the integral $I(a)$, Eq. (58), leads to

$$H_0 [(\phi(a) - \phi_0) + (\xi(a) - \xi_0)] \approx -\frac{2\sqrt{2A}}{1 + \tilde{h}} \left[\left(\frac{1 + \tilde{h}}{a} - \tilde{h} \right)^{1/2} - 1 \right]. \quad (65)$$

Inverting this expression and substituting in the above equation (64), we get

$$V(\phi, \xi) \approx V_0 + (5A - 6B) \left[1 - \frac{1 + \tilde{h}}{\left\{ 1 - \frac{(1 + \tilde{h})H_0}{2\sqrt{2A}} [(\phi - \phi_0) + (\xi - \xi_0)] \right\}^2 + \tilde{h}} \right]. \quad (66)$$

The variations of the exact and approximated forms of $H_0 [(\phi - \phi_0) + (\xi - \xi_0)]$ with the scale factor a , as well as the functional variation of the approximated $[V(\phi, \xi) - V_0]$, are shown in the upper panels (left and right respectively) of Fig. 6. The approximation is found to hold for a fairly large range $0.7 \lesssim a \lesssim 1.4$. The approximated $[V(\phi, \xi) - V_0]$, which has been plotted

¶ Note that Eq. (57) cannot be used now, because the approximation does not hold for $a = 0$.

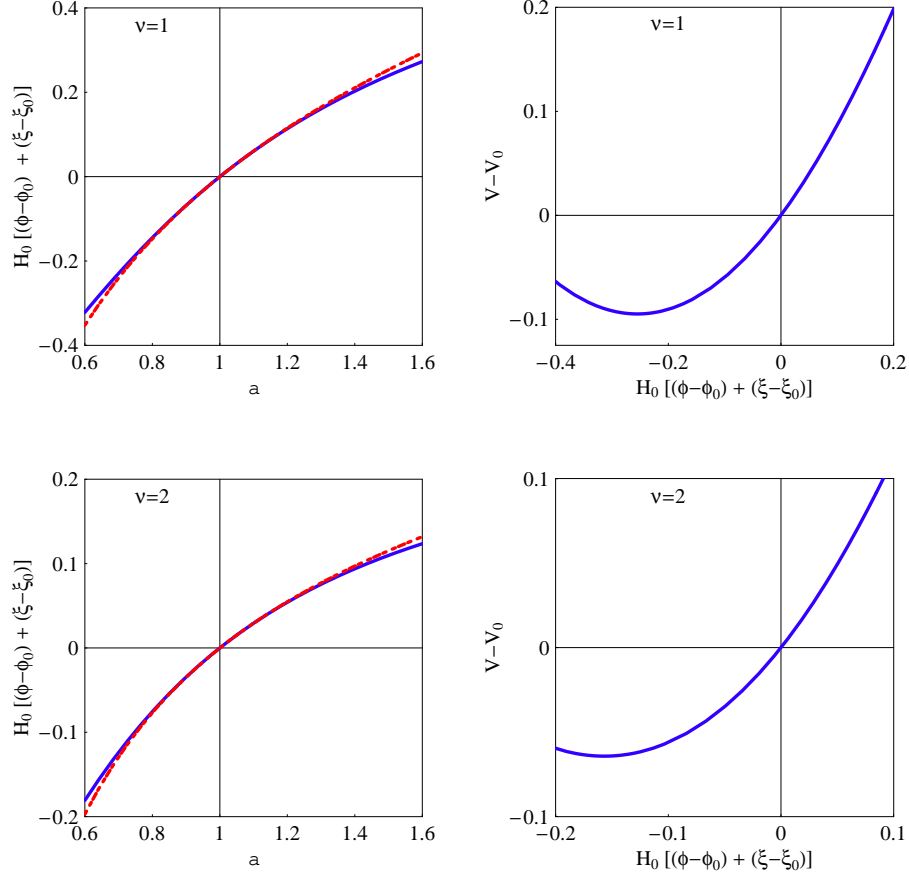


Figure 6. Exact and approximate (solid and dashed lines) variations of $H_0[(\phi - \phi_0) + (\xi - \xi_0)]$ with the scale factor $a(\approx 1)$, as well as the approximated functional variation $[V(\phi, \xi) - V_0]$, are shown for the choices $\nu = 1$ (upper panels) and $\nu = 2$ (lower panels). The approximation is found to be good in the range $0.7 \lesssim a \lesssim 1.4$ for both $\nu = 1$ and 2. Within this range $V - V_0$ has a minimum at $H_0[(\phi - \phi_0) + (\xi - \xi_0)] \simeq -0.25$ (for $\nu = 1$) and $\simeq -0.15$ (for $\nu = 2$).

for this range of validity, has a minimum ($\simeq -0.1$) at $H_0[(\phi - \phi_0) + (\xi - \xi_0)] \sim -0.25$. The overall profile of the approximated $V - V_0$ is similar to the exact variation of $V - V_0$ with a (shown in Fig. 4) in the range $0.7 < a < 1.4$ where the approximation is found to be valid.

For $\nu = 2$: The approximation of the expression (34) for the potential V is given by

$$V(a) = V_0 + 2(2A - 3B)(1 - a), \quad (67)$$

and by evaluating the integral $I(a)$ given by Eq. (58), approximately, one finds

$$H_0[(\phi(a) - \phi_0) + (\xi(a) - \xi_0)] \approx \sqrt{\frac{2A}{1 + \tilde{h}}} \left[\left\{ \sqrt{1 - \frac{\tilde{h}}{1 + \tilde{h}}} - \frac{1}{a} \sqrt{1 - \frac{\tilde{h}a}{1 + \tilde{h}}} \right\} \right]$$

$$+ \frac{\tilde{h}}{1+\tilde{h}} \left\{ \tanh^{-1} \left(\sqrt{1 - \frac{\tilde{h}}{1+\tilde{h}}} \right) - \tanh^{-1} \left(\sqrt{1 - \frac{\tilde{h}a}{1+\tilde{h}}} \right) \right\}. \quad (68)$$

This expression cannot be inverted to get the scale factor a as a function of $H_0 [(\phi - \phi_0) + (\xi - \xi_0)]$, and hence obtain the expression for the analytic functional variation of the approximated $V(\phi, \xi)$. However, one may find the parametric plot of the approximated $[V(\phi, \xi) - V_0]$ versus $H_0 [(\phi - \phi_0) + (\xi - \xi_0)]$ using the above equations (67) and (68). Such a plot is shown in the lower right panel of Fig. 6. $[V(\phi, \xi) - V_0]$ varies in a similar way as for $\nu = 1$ (see the upper right panel of Fig. 6), however the minimum value is higher and the minimum is reached at a value $H_0 [(\phi - \phi_0) + (\xi - \xi_0)] \simeq -0.15$, greater than that for $\nu = 1$. The lower left panel of Fig. 6) shows how the exact and approximate forms of $H_0 [(\phi - \phi_0) + (\xi - \xi_0)]$ vary with the scale factor a . Similar to the case $\nu = 1$ (upper left), we find that the approximation remains valid in a fairly large region $0.7 \lesssim a \lesssim 1.4$ as well for $\nu = 2$ (lower left).

Finally, it should be mentioned here that although we have expressed the potential V approximately as a function of $(\phi + \xi)$ for both $a \ll 1$ and $a \simeq 1$ (see the Eqs. (61) and (66)), strictly speaking this cannot be true at all epochs. Indeed, if V is exactly a function of $(\phi + \xi)$, i.e., $\partial V / \partial \phi = \partial V / \partial \xi$, then the ansatz (30) becomes inconsistent with the scalar field equations of motion (19), given in sec. 3, and all our above results are invalid. The exact form of the potential V , which we are studying in a later work (in preparation) [54], should therefore be asymmetric in ϕ and ξ (at least to their linear order) in order the model to be consistent.

6. Conclusions

We have thus explored the plausible crossing of the cosmological constant (Λ) barrier by the dark energy equation of state parameter w_x in a fairly simple set-up of two canonical (quintessence-type) scalar fields with a mutual kinetic interaction. Such a crossing, which has been a big problem in many scalar field DE models, is shown to be realized with a specific form of the kinetic interaction and with the requirement that the dynamical part of total DE Hamiltonian is positive definite, so that the model is quantum mechanically consistent. Classical stability of the model is also guaranteed as the squares of the sound speeds corresponding to the adiabatic and entropy perturbation modes are positive definite.

Under certain limiting conditions, the specific form of the kinetic interaction, which we study, can be shown to have originated from a higher dimensional two-scalar DBI action, that appears in the string theoretic scenario [44]. Such a kinetic interaction provides additional flexibility in w_x (apart from those provided by the usual kinetic terms of the scalar fields), so that the Λ -barrier (i.e., $w_x = -1$) could be crossed at a particular epoch.

Joint constraints on the parameters of the model by the SN+CMB+BAO data due to the SN Search Team [8], WMAP [14] and SDSS [15], show that w_x has most likely crossed -1 at a recent red-shift $z = z_c$ ($0.215 \leq z_c \leq 0.245$), and its value w_{0x} at present is less than -1 ($-1.123 \leq w_{0x} \leq -1.077$). On the other hand, the transition from the decelerated phase of expansion of the universe to the accelerated phase takes place between $0.562 < z < 0.603$. All these results are fairly consistent with the model-independent estimates

with the SN+CMB+BAO data in ref. [14]. Additionally, we also observe that the dark energy density (best fit with the observational data) nearly follows the matter density (i.e., exhibits a similar fall-off with the scale factor a , as the latter) at early epochs, until exceeding it very recently. This apparently could provide a resolution to the coincidence problem (that is associated with the cosmological constant). Extrapolations to future epochs also show that the best fit dark energy density increases fairly slowly even at a fairly large scale factor, implying that singularities in finite future may plausibly be avoided in our model.

The numerical reconstruction of functional forms of the scalar fields and the scalar potential, using the best fit values of the model parameters, shows smooth variations with the scale factor a , although analytically the exact form of the potential as function of the fields is very difficult to obtain. Working out therefore the approximate solutions for the scalar fields in the early universe and near the present epoch, we have obtained approximate analytic functional forms of the potential in terms of the scalar fields, in these regimes. Such analytic forms also exhibit the same smooth nature as the numerically reconstructed potential.

Some interesting questions that arise in the context of the present model are in order:

- Can one unify dark matter and dark energy in the general framework of a kinetically interacting double or multi-scalar theory, instead of treating them separately as in this model?
- Can we generically determine for kinetically interacting double or multi-quintessence model, the exact form of the scalar potential, which could lead to the Λ -barrier crossing as well as the dark matter tracking (by DE)? If so, then could it be ascertained whether such a potential belongs the class of tracking or scaling potentials that arise in generic k-essence theories?
- Can we have in the context of a kinetically interacting double or multi-quintessence model, the assisted accelerated solutions, which have been shown to exist generically for the multi-field k-essence models admitting scaling solutions [55]?
- Can we ascertain the status of the future singularities, if any, in the context of kinetically interacting double-quintessence models, generically, i.e., by not just resorting to a particular ansatz to solve for the field equations? Or, can we generically ascertain whether or not the cosmic super-acceleration ($w_x < -1$ regime) is always eternal (as in the present model) for kinetically interacting two-field quintessence?

Works addressing some of these questions are in progress [54], which we hope to report soon.

Acknowledgments

The author acknowledges useful discussions with the members of the theoretical physics group of University of Lethbridge, and especially to Saurya Das for many helpful remarks and suggestions. This work is supported by the Natural Sciences and Engineering Research Council of Canada.

Appendix: Kinetic interaction from a two-field DBI perspective

The Dirac-Born-Infeld (DBI) multi-scalar Lagrangian is particularly important in view of the notion acquired from string theory that our observable four dimensional world may be looked upon as being a warped D3-brane embedded in a higher dimensional (bulk) space-time [56]. The general expression for such a Lagrangian in an effective four dimensional theory is given by [41, 42]:

$$P = \gamma \left(1 - \sqrt{\mathcal{D}} \right) - U(\phi^I), \quad (69)$$

where $\phi^I (I = 1, 2, \dots)$ are a set of scalar fields, which from the bulk point of view, correspond to the coordinates of the brane in the extra dimensions, and $U(\phi^I)$ is the multi-field potential due to the interaction of the brane with bulk fields or with fields on other branes. \mathcal{D} is the determinant of induced metric on the brane, given by

$$\mathcal{D} = \det \left(\delta_\mu^\nu + \gamma^{-1} \mathcal{G}_{IJ} \partial_\mu \phi^I \partial^\nu \phi^J \right), \quad (70)$$

where \mathcal{G}_{IJ} is the field space metric, which is proportional to the extra dimensional metric living in the bulk, and γ is a coupling parameter, that appears by virtue of the warping of the D3-brane in the bulk. Both \mathcal{G}_{IJ} and γ could generally be functions of the fields ϕ^I , and in a homogeneous FRW background the above expression for \mathcal{D} takes the form [41, 42]:

$$\mathcal{D} = 1 - 2\gamma^{-1} \mathcal{G}_{IJ} X^{IJ}, \quad X^{IJ} = \frac{\dot{\phi}^I \dot{\phi}^J}{2}. \quad (71)$$

Now, for a configuration of two fields $\phi^I := \{\phi, \xi\}$, assuming γ and \mathcal{G}_{IJ} to be constants (for all I, J), we can write

$$\mathcal{D} = 1 - \gamma^{-1} \left(\mathcal{G}_{11} \dot{\phi}^2 + \mathcal{G}_{22} \dot{\xi}^2 + 2\mathcal{G}_{12} \dot{\phi} \dot{\xi} \right). \quad (72)$$

Rescaling ϕ and ξ such that both the metric components \mathcal{G}_{11} and \mathcal{G}_{22} are effectively set to unity, we get

$$\mathcal{D} = 1 - \frac{\dot{\phi}^2 + \dot{\xi}^2}{\gamma} - \frac{\beta}{2} \dot{\phi} \dot{\xi}, \quad \text{where } \beta = \frac{4\mathcal{G}_{12}}{\gamma} = \text{constant}. \quad (73)$$

Under the assumption:

$$\gamma \gg \mathcal{G}_{12} \gg 1 \quad \Rightarrow \quad \beta \ll 1, \quad \text{but } \gamma^{-1} \ll \beta, \quad (74)$$

one can write⁺

$$\sqrt{\mathcal{D}} = - \frac{\dot{\phi}^2 + \dot{\xi}^2}{2\gamma} + \sqrt{1 - \frac{\beta}{2} \dot{\phi} \dot{\xi}} + \mathcal{O}\left(\frac{\beta}{\gamma}\right). \quad (75)$$

Substituting this in Eq. (69), and neglecting the $\mathcal{O}(\beta/\gamma)$ and higher order terms, we finally obtain

$$P = \frac{\dot{\phi}^2 + \dot{\xi}^2}{2} - \gamma \sqrt{1 - \frac{\beta}{2} \dot{\phi} \dot{\xi}} - V(\phi, \xi). \quad (76)$$

⁺ Note that in this paper we have typically set $\gamma = 10^4$ and with $\mathcal{G}_{12} = 10^2$, it implies $\beta = 4\mathcal{G}_{12}/\gamma = 10^{-2} \ll 1$ (but $\gg \gamma^{-1}$), as per the assumption (74) [see sec. 5].

This is the same as the KIDQ Lagrangian (14) considered in sec. 3; $V(\phi, \xi) = U(\phi, \xi) - \gamma$ being the effective (shifted) two-scalar potential.

Stability criterion: In general multiple scalar field models, the cosmological perturbations of scalar type are divided into: (i) the adiabatic (instantaneous) modes, which are fluctuations along the field space trajectory, and (ii) the entropy modes, which are orthogonal to the field space trajectory [57]. The squares of the speeds of propagation of both these modes should be positive definite in order that the underlying model is cosmologically stable.

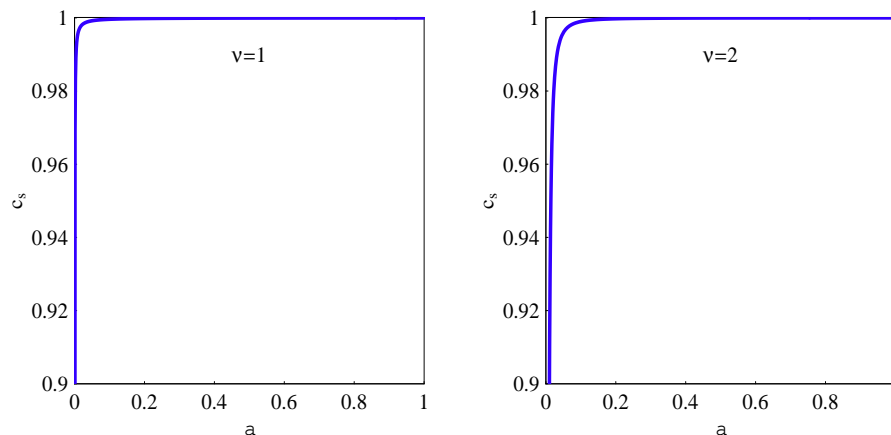


Figure 7. Plots of the KIDQ sound speed c_s (assumed to be isotropic) as a function of the scale factor a , for the choices $\nu = 1$ and $\nu = 2$. Except at very early epochs ($a \ll 1$), the sound speed is found to be extremely close to unity (i.e., the speed of light), for both the choices.

For multi-scalar DBI models [41, 42], the adiabatic and entropy modes are shown to be isotropic, i.e., they propagate with the same (sound) speed c_s equal to $\sqrt{\mathcal{D}}$. Since the KIDQ Lagrangian is an approximation of the two-scalar DBI Lagrangian under the assumption (74), one may intuitively consider this isotropy of the perturbation modes exists in the case of KIDQ as well, and that the effective sound speed for KIDQ to be $c_s = \sqrt{\mathcal{D}}$, given by Eq. (75). Obviously, as shown in Fig. 7, this sound speed (and as such its square) is positive definite and very close to unity (speed of light) for both $\nu = 1$ and $\nu = 2$, since the γ^{-1} and β terms in Eq. (75) are very small compared to unity.

More generally of course, if we treat KIDQ as an exact model (i.e., not an approximation of DBI), then a rigorous analysis following the general formalism worked out in [42], shows that the sound speeds corresponding to the adiabatic and entropy modes do actually differ. However, the difference is very slight for the values of the parameters β, γ used in this paper, and the sound speeds are still positive definite and close to unity [54].

References

- [1] S. J. Perlmutter *et al* [Supernova Cosmology Project collaboration], Bull. Am. Astron. Soc. **29** 1351 (1997) [astro-ph/9812473];

- A. G. Riess *et al* [Supernova Search Team collaboration], *Astron. J.* **116** 1009 (1998) [astro-ph/9805201];
S. J. Perlmutter *et al*, *Astrphys. J.* **517** 565 (1999) [astro-ph/9812133].
- [2] J. L. Tonry *et al* [Supernova Search Team collaboration], *Astrophys. J.* **594** 1 (2003) [astro-ph/0305008];
R. A. Knop *et al* [Supernova Search Team collaboration], *Astrophys. J.* **598** 102 (2003) [astro-ph/0309368];
B. J. Baris *et al*, *Astrophys. J.* **602** 571 (2004) [astro-ph/0310843].
- [3] A. G. Riess *et al* [Supernova Search Team collaboration], *Astrophys. J.* **607** 665 (2004) [astro-ph/0402512].
- [4] A. G. Riess *et al* [Supernova Search Team collaboration], *Astrophys. J.* **659** 98 (2007) [astro-ph/0611572].
- [5] P. Astier *et al* [SNLS collaboration], *Astron. Astrophys.* **447** 31 (2006) [astro-ph/0510447].
- [6] T. M. Davis *et al*, *Astrophys. J.* **666** 716 (2007) [astro-ph/0701510].
- [7] G. Miknaitis *et al* [ESSENCE collaboration], *Astrophys. J.* **666** 674 (2007) [astro-ph/0701043];
W. M. Wood-Vasey *et al* [ESSENCE collaboration], *Astrophys. J.* **666** 694 (2007) [astro-ph/0701041].
- [8] M. Kowalski *et al*, *Astrophys. J.* **686** 749 (2008) [arXiv:0804.4142];
- [9] D. Rubin *et al*, arXiv:0807.1108.
- [10] S. Capozziello, V. F. Cardone, S. Carloni and A. Troisi, *Int. J. Mod. Phys. D* **12** 1969 (2003) [astro-ph/0307018];
S. M. Carroll, V. Duvvuri, M. Trodden and M. S. Turner, *Phys. Rev. D* **70** 043528 (2004) [astro-ph/0306438];
S. Nojiri and S. D. Odintsov, *Phys. Rev. D* **68** 123512 (2003) [hep-th/0307288];
T. Chiba, *Phys. Lett. B* **575** 1 (2003) [astro-ph/0307338];
S. M. Carroll, A. De Felice, V. Duvvuri, D. A. Easson, M. Trodden and M. S. Turner, *Phys. Rev. D* **71** 063513 (2005) [astro-ph/0410031];
S. Carloni, P. K. S. Dunsby, S. Capozziello and A. Troisi, *Class. Quant. Grav.* **22** 4839 (2005) [gr-qc/0410046];
L. Amendola, D. Polarski and S. Tsujikawa, *Phys. Rev. Lett.* **98** 131302 (2007) [astro-ph/0603703];
A. V. Frolov, *Phys. Rev. Lett.* **101** 061103 (2008) [arXiv:0803.2500].
- [11] D. L. Wiltshire, *Phys. Rev. Lett.* **99** 251101 (2007) [arXiv:0709.0732];
D. L. Wiltshire, *Int. J. Mod. Phys. D* **17** 641 (2008) [arXiv:0712.3982];
D. L. Wiltshire, *New J. Phys.* **9** 377 (2007) [gr-qc/0702082].
- [12] D. N. Spergel *et al* [WMAP Collaboration], *Astrophys. J. Suppl.* **148** 175 (2003) [astro-ph/0302209];
C. L. Bennet *et al* [WMAP Collaboration], *Astrophys. J. Suppl.* **148** 1 (2003) [astro-ph/0302207];
M. R.olta *et al* [WMAP Collaboration], *Astrophys. J.* **608** 10 (2004) [astro-ph/0305097];
- [13] L. Page *et al* [WMAP Collaboration], *Astrophys. J. Suppl.* **170** 335 (2007) [astro-ph/0603450];
D. N. Spergel *et al* [WMAP Collaboration], *Astrophys. J. Suppl.* **170** 377 (2007) [astro-ph/0603449];
- [14] E. Komatsu *et al* [WMAP Collaboration], arXiv:0803.0547;
G. Hinshaw *et al* [WMAP Collaboration], arXiv:0803.0732;
J. Dunkley *et al* [WMAP Collaboration], arXiv:0803.0586;
R. Hill *et al* [WMAP Collaboration], arXiv:0803.0570;
B. Gold *et al* [WMAP Collaboration], arXiv:0803.0715;
E. L. Wright *et al* [WMAP Collaboration], arXiv:0803.0577;
M. R.olta *et al* [WMAP Collaboration], arXiv:0803.0593;
See also L. Page, The newsletter of the Topical Group on Gravitation, *Am. Phys. Soc.*, No. 32, Fall 2008 (<http://axion.physics.ubc.ca/hyperspace/mog32.pdf>), for a summary of WMAP 5 year results.
- [15] D. Eisenstein *et al* [SDSS collaboration], *Astrophys. J.* **633** 560 (2005) [astro-ph/0501171];
M. Tegmark *et al* [SDSS collaboration], *Phys. Rev. D* **74** 123507 (2006) [astro-ph/0608632].
- [16] S. M. Carroll, *Living Rev. Rel.* **4** 1 (2001) [astro-ph/0004075];
T. Padmanabhan, *Phys. Rept.* **380** 235 (2006) [hep-th/0212290],
J. Polchinski, hep-th/0603249;
L. M. Krauss and R. J. Scherrer, *Gen. Rel. Grav.* **39** 1545 (2007) [arXiv:0704.0221].
- [17] R. R. Caldwell, R. Dave and P. J. Steinhardt, *Phys. Rev. Lett.* **80** 1582 (1998) [astro-ph/9708069];
S. M. Carroll, *Phys. Rev. Lett.* **81** 3067 (1998) [astro-ph/9806099];

- E. J. Copeland, A. R. Liddle and D. Wands, Phys. Rev. **D57** 4686 (1998) [gr-qc/9711068];
A. R. Liddle and R. J. Scherrer, Phys. Rev. **D59** 023509 (1999) [astro-ph/9809272].
- [18] I. Zlatev, L. -M. Wang and P. J. Steinhardt, Phys. Rev. Lett. **82** 896 (1999) [astro-ph/9807002];
P. J. Steinhardt, L. -M. Wang and I. Zlatev, Phys. Rev. **D59** 123504 (1999) [astro-ph/9812313];
R. R. Caldwell and E. V. Linder, Phys. Rev. Lett. **95** 141301 (2005) [astro-ph/0505494];
R. J. Scherrer, Phys. Rev. **D73** 043502 (2006) [astro-ph/0509890];
T. Chiba, Phys. Rev. **D73** 063501 (2006) [astro-ph/0510598].
- [19] C. Armendariz-Picon, V. F. Mukhanov and P. J. Steinhardt, Phys. Rev. Lett. **85** 4438 (2000) [astro-ph/0004134];
C. Armendariz-Picon, V. F. Mukhanov and P. J. Steinhardt, Phys. Rev. **D63** 103510 (2001) [astro-ph/0006373];
C. Armendariz-Picon, T. Damour and V. F. Mukhanov, Phys. Lett. **B458** 209 (1999) [hep-th/9904075];
T. Chiba, T. Okabe and M. Yamaguchi, Phys. Rev. **D62** 023511 (2000) [astro-ph/9912463];
T. Chiba, Phys. Rev. **D66** 063514 (2002) [astro-ph/0206298].
- [20] M. Malquarti, E. J. Copeland, A. R. Liddle and M. Trodden, Phys. Rev. **D67** 123503 (2003) [astro-ph/0302279];
M. Malquarti, E. J. Copeland and A. R. Liddle, Phys. Rev. **D68** 023512 (2003) [astro-ph/0304277];
J. M. Aguirregabiria, L. P. Chimento and R. Lazkoz, Phys. Rev. **D70** 023509 (2004) [astro-ph/0403157];
L. P. Chimento and A. Feinstein, Mod. Phys. Lett. **A19** 761 (2004) [astro-ph/0305007];
L. P. Chimento, Phys. Rev. **D69** 123517 (2004) [astro-ph/0311613].
- [21] A. Y. Kamenshchik, U. Moschella and V. Pasquier, Phys. Lett. **B511** 265 (2001) [gr-qc/0103004];
N. Bilic, G. B. Tupper and R. D. Viollier, Phys. Lett. **B535** 17 (2002) [astro-ph/0111325];
M. C. Bento, O. Bertolami and A. A. Sen, Phys. Rev. **D66** 043507 (2002) [gr-qc/0202064].
- [22] T. Padmanabhan, Gen. Rel. Grav. **40** 529 (2008) [gr-qc/0202064];
E. J. Copeland, M. Sami and S. Tsujikawa, Int. J. Mod. Phys. **D15** 1753 (2006) [hep-th/0603057];
P. J. E. Peebles and B. Ratra, Rev. Mod. Phys. **75** 559 (2003) [astro-ph/0207347];
V. Sahni and A. A. Starobinsky, Int. J. Mod. Phys. **D9** 373 (2000) [astro-ph/9904398].
- [23] B. Feng, X. L. Wang and X. M. Zhang, Phys. Lett. **B607** 35 (2005) [astro-ph/0404224];
Z. K. Guo, Y. -S. Piao, X. M. Zhang and Y. Z. Zhang, Phys. Lett. **B608** 177 (2005) [astro-ph/0410654];
B. Feng, M. Li, Y. -S. Piao and X. Zhang, Phys. Lett. **B634** 101 (2006) [astro-ph/0407432];
R. Lazkoz and G. Leon, Phys. Lett. **B638** 303 (2006) [astro-ph/0602590];
R. Lazkoz, G. Leon and I. Quiros, Phys. Lett. **B649** 103 (2007) [astro-ph/0701353];
Y. -F. Cai, M. Li, J. X. Lu, Y. -S. Piao, T. Qiu and X. Zhang, Phys. Lett. **B651** 1 (2007) [hep-th/0701016];
Y. -F. Cai, H. Li, Y. -S. Piao, X. -M. Zhang, Phys. Lett. **B646** 141 (2007) [gr-qc/0609039].
- [24] R. R. Caldwell, Phys. Lett. **B545** 23 (2002) [astro-ph/9908168];
N. Arkani-Hamed, P. Creminelli, S. Mukohyama and M. Zaldarriaga, JCAP **0404** 001 (2004) [hep-th/0312100];
F. Piazza and S. Tsujikawa, JCAP **0407** 004 (2004) [hep-th/0405054];
L. P. Chimento and R. Lazkoz, Phys. Rev. Lett. **91** 211301 (2003) [gr-qc/0307111];
S. Tsujikawa, Class. Quant. Grav. **20** 1991 (2003) [hep-th/0302181];
L. Perivolaropoulos, Phys. Rev. **D71** 063503 (2005) [astro-ph/0412308];
S. Nesseris and L. Perivolaropoulos, Phys. Rev. **D70** 123529 (2004) [astro-ph/0410309].
- [25] J. M. Cline, S. Y. Jeon and G. D. Moore, Phys. Rev. **D70** 043543 (2004) [hep-ph/0311312].
- [26] R. R. Caldwell, M. Kamionkowski and N. N. Weinberg, Phys. Rev. Lett. **91** 071301 (2003) [astro-ph/0302506].
- [27] S. Nojiri, S. D. Odintsov and S. Tsujikawa, Phys. Rev. **D71** 063004 (2005) [hep-th/0501025].
- [28] S. M. Carroll, M. Hoffman and M. Trodden, Phys. Rev. **D68** 023509 (2003) [astro-ph/0301273].
- [29] B. Boisseau, G. Esposito-Farese, D. Polarski and A. A. Starobinsky, Phys. Rev. Lett. **85** 2236 (2000) [gr-qc/0001066];
G. Esposito-Farese and D. Polarski, Phys. Rev. **D63** 063504 (2001) [gr-qc/0009034];
L. Perivolaropoulos, JCAP **0510** 001 (2005) [astro-ph/0504582];

- S. Nesseris and L. Perivolaropoulos, Phys. Rev. **D73** 103511 (2006) [astro-ph/0602053].
- [30] V. Sahni and Y. Shtanov, JCAP **0311** 014 (2003) [astro-ph/0202346];
V. Sahni and Y. Shtanov, Phys. Rev. **D71** 084018 (2005) [astro-ph/0410221].
- [31] L. P. Chimento and R. Lazkoz, Phys. Lett. **B639** 591 (2006) [astro-ph/0604090].
- [32] S. Sur and S. Das, JCAP **0901** 007 (2009) [arXiv:0806.4368].
- [33] See for example L. Amendola and S. Tsujikawa, Phys. Lett. **B660** 125 (2008) [arXiv:0705.0396] and references therein.
- [34] N. Arkani-Hamed, P. Creminelli, S. Mukohyama and M. Zaldariagga, JCAP **0404** 001 (2004) [hep-th/0312100];
F. Piazza and S. Tsujikawa, JCAP **0407** 004 (2004) [hep-th/0405054].
- [35] V. K. Onemli and R. P. Woodard, Class. Quant. Grav. **19** 4607 (2002) [gr-qc/0204065];
V. K. Onemli and R. P. Woodard, Phys. Rev. **D70** 107301 (2004) [gr-qc/0406098];
E. O. Kahya and V. K. Onemli, Phys. Rev. **D76** 043512 (2007) [gr-qc/0612026].
- [36] S. Nojiri, S. D. Odintsov and S. Tsujikawa, Phys. Rev. **D71** 063004 (2005) [hep-th/0501025];
B. Gumjudpai, T. Naskar, M. Sami and S. Tsujikawa, JCAP **0506** 007 (2005) [hep-th/0502191].
- [37] H. Wei, R. -G. Cai and D. -F. Zeng, Class. Quant. Grav. **22** 3189 (2005) [hep-th/0501160];
H. Wei and R. -G. Cai, Phys. Rev. **D72** 123507 (2005) [astro-ph/0509328];
H. Wei, N. -N. Tang and S. N. Zhang, Phys. Rev. **D75** 043009 (2007) [astro-ph/0612746].
- [38] A. A. Andrianov, F. Cannata and A. Y. Kamenshchik, Phys. Rev. **D72** 043531 (2005) [gr-qc/0505087];
F. Cannata and A. Y. Kamenshchik, Int. J. Mod. Phys. **D16** 1683 (2007) [gr-qc/0603129];
A. K. Sanyal, arXiv:0710.3486.
- [39] S. Capozziello, S. Nojiri and S. D. Odintsov, Phys. Lett. **B632** 597 (2006) [hep-th/0507182];
S. Nojiri and S. D. Odintsov, Gen. Rel. Grav. **38** 1285 (2006) [hep-th/0506212].
- [40] A. Vikman, Phys. Rev. **D71** 023515 (2005) [astro-ph/0407107].
- [41] D. Langlois, S. Renaux-Petel, D. A. Steer and T. Tanaka, Phys. Rev. Lett. **101** 061301 (2008) [arXiv:0804.3139];
- [42] D. Langlois, S. Renaux-Petel, D. A. Steer and T. Tanaka, Phys. Rev. **D78** 063523 (2008) [arXiv:0806.0336].
- [43] D. Langlois and S. Renaux-Petel, JCAP **0804** 017 (2008) [arXiv:0801.1085];
- [44] J. M. Cline, hep-th/0612129;
A. Sen, Phys. Rev. **D68** 066008 (2003) [hep-th/0303057];
A. Sen, JHEP **0207** 065 (2002) [hep-th/0203265];
A. Sen, JHEP **0204** 048 (2002) [hep-th/0203211];
E. Silverstein and D. Tong, Phys. Rev. **D70** 103505 (2004) [hep-th/0310221];
M. Alishahiha, E. Silverstein and D. Tong, Phys. Rev. **D70** 123505 (2004) [hep-th/0404084].
- [45] S. Sur, in preparation.
- [46] M. Chevallier and D. Polarski, Int. J. Mod. Phys. **D10** 213 (2001) [gr-qc/0009008];
E. V. Linder, Phys. Rev. Lett. **90** 091301 (2003) [astro-ph/0208512].
- [47] U. Alam, V. Sahni, T. D. Saini and A. A. Starobinsky, Mon. Not. Roy. Astron. Soc. **354** 275 (2004) [astro-ph/0311364].
- [48] M. Visser, Class. Quant. Grav. **21** 2603 (2004) [gr-qc/0309109].
- [49] C. A. Shapiro and M. S. Turner, Astrophys. J. **649** 563 (2006) [astro-ph/0512586];
H. K. Jassal, J. S. Bagla and T. Padmanabhan, Mon. Not. Roy. Astron. Soc. **356** L11 (2005) [astro-ph/0404378];
T. R. Choudhury and T. Padmanabhan, Astron. Astrophys. **429** 807 (2005) [astro-ph/0311622];
E. V. Linder and D. Huterer, Phys. Rev. **D72** 043509 (2005) [astro-ph/0505330];
C. Wetterich, Phys. Lett. **B594**, 17 (2004) [astro-ph/0403289];
E. V. Linder, arXiv:0708.0024;
F. C. Carvalho, J. S. Alcaniz, J. A. S. Lima and R. Silva, Phys. Rev. Lett. **97** 081301 (2006) [astro-ph/0608439];
J. S. Alcaniz and J. A. S. Lima, Phys. Rev. **D72** 063516 (2005) [astro-ph/0507372];
R. -G. Cai and A. Wang, JCAP **0503** 002 (2005) [hep-th/0411025];

- Y. G. Gong and A. Wang, Phys. Rev. **D75** 043520 (2007) [astro-ph/0612196];
A. A. Sen, Phys. Rev. **D77** 043508 (2008) [arXiv:0708.1072].
- [50] S. Nesseris and L. Perivolaropoulos, JCAP **0701** 018 (2007) [astro-ph/0610092];
S. Nesseris and L. Perivolaropoulos, Phys. Rev. **D72** 123519 (2005) [astro-ph/0511040];
V. Sahni and A. A. Starobinsky, Int. J. Mod. Phys. **D15** 2105 (2006) [astro-ph/0610026];
U. Alam, V. Sahni and A. A. Starobinsky, JCAP **0702** 011 (2007) [astro-ph/0612381];
L. P. Chimento, R. Lazkoz, R. Maartens and I. Quiros, JCAP **0609** 004 (2006) [astro-ph/0605450];
S. Fay and R. Tavakol, arXiv:0801.2128.
- [51] L. Perivolaropoulos, Phys. Rev. **D71** 063503 (2005) [astro-ph/0412308];
E. Di Pietro and J. F. Claeskens, Mon. Not. Roy. Astron.Soc. **341** 1299 (2003) [astro-ph/0207332].
- [52] H. Wei, arXiv:0809.0057.
- [53] Y. Wang and P. Mukherjee, Astrophys. J. **650** 1 (2006) [astro-ph/0604051].
- [54] S. Sur, in preparation.
- [55] S. Tsujikawa, Phys. Rev. **D73** 103504 (2006) [arXiv:hep-th/0601178].
- [56] See for example, A. Kehagias and E. Kiritsis, JHEP **9911** 022 (1999) [hep-th/9910174], and references therein.
- [57] C. Gordon, D. Wands, B. A. Bassett and R. Maartens, Phys. Rev. **D63** 023506 (2001) [astro-ph/0009131].